HHS Public Access

Author manuscript

Annu Rev Biochem. Author manuscript; available in PMC 2015 December 16.

Published in final edited form as:

Annu Rev Biochem. 2015 ; 84: 519–550. doi:10.1146/annurev-biochem-060614-034411.

Natural Photoreceptors as a Source of Fluorescent Proteins, Biosensors, and Optogenetic Tools

Daria M. Shcherbakova[1,*], **Anton A. Shemetov**[1,*], **Andrii A. Kaberniuk**[1,*], and **Vladislav V. Verkhusha**[1,2]

Vladislav V. Verkhusha: vladislav.verkhusha@einstein.yu.edu

[1]Department of Anatomy and Structural Biology, Albert Einstein College of Medicine, Bronx, New York 10461 [2]Department of Biochemistry and Developmental Biology, Faculty of Medicine, University of Helsinki, Helsinki 00290, Finland

Abstract

Genetically encoded optical tools have revolutionized modern biology by allowing detection and control of biological processes with exceptional spatiotemporal precision and sensitivity. Natural photoreceptors provide researchers with a vast source of molecular templates for engineering of fluorescent proteins, biosensors, and optogenetic tools. Here, we give a brief overview of natural photoreceptors and their mechanisms of action. We then discuss fluorescent proteins and biosensors developed from light-oxygen-voltage-sensing (LOV) domains and phytochromes, as well as their properties and applications. These fluorescent tools possess unique characteristics not achievable with green fluorescent protein–like probes, including near-infrared fluorescence, independence of oxygen, small size, and photo-sensitizer activity. We next provide an overview of available optogenetic tools of various origins, such as LOV and BLUF (blue-light-utilizing flavin adenine dinucleotide) domains, cryptochromes, and phytochromes, enabling control of versatile cellular processes. We analyze the principles of their function and practical requirements for use. We focus mainly on optical tools with demonstrated use beyond bacteria, with a specific emphasis on their applications in mammalian cells.

Keywords

optogenetics; phytochrome; bacteriophytochrome; BphP; CRY2; iRFP; LOV domain

INTRODUCTION

Recent progress in the development of genetically encoded molecules for life science optical technologies, such as fluorescent proteins (FPs), biosensors, and optogenetic tools (OTs), became possible with the use of natural photoreceptors as building blocks for protein

*These authors contributed equally to this review.

DISCLOSURE STATEMENT

The authors are not aware of any affiliations, memberships, funding, or financial holdings that might be perceived as affecting the objectivity of this review.

engineering. These molecular tools provide new possibilities to image, detect, and control biological processes using light with exceptional spatiotemporal precision.

Natural photoreceptors play essential roles in many organisms, including plants, bacteria, fungi, and higher eukaryotes. To sense light, photoreceptors typically incorporate an exogenous cofactor molecule, called a chromophore, that absorbs light and transmits energy to a protein backbone. As a result of the photochemical transformations in a chromophore and the conformational changes in a protein backbone, receptor activation and signaling propagation occur. Many natural photoreceptors consist of an N-terminal photosensory unit and a coupled C-terminal effector domain, which frequently exhibit enzymatic activity, although there are receptors with N-terminal effector domains (1–3). A photocycle in many photoreceptors is reversible.

Photoreceptors employed in the design of optical tools can be divided into several classes according to their chromophores and light-sensing protein domains (Figure 1). The UV- and blue-light-sensing (∼300–500 nm) flavoproteins, such as receptors with light-oxygen-voltage-sensing (LOV) domains; blue-light-utilizing flavin adenine dinucleotide (BLUF) domains; and cryptochromes incorporate flavin mononucleotide (FMN) or flavin adenine dinucleotide (FAD) as a chromophore (4, 5). Another class of photoreceptors, called xanthopsins, also sense UV and blue light. These proteins incorporate 4-hydroxy–cinnamic acid as a chromophore. Xanthopsins, however, have not been extensively used to engineer optical probes, because they do not incorporate the chromophore autocatalytically. Thus, they are not covered in this review. A versatile family of receptors, called opsins, sense blue, green, and red light and incorporate retinal as a chromophore. Far-red- and near-infrared (NIR)-light-sensing photoreceptors, called phytochromes, utilize various linear tetrapyrrole bilins as chromophores (Figure 1).

The first photoreceptors widely explored as OTs were microbial opsins, acting as light-gated cation channels and ion pumps. The use of opsins has already transformed research in neuroscience, where they have been applied to activate and silence specific cells with exceptional spatiotemporal precision. OTs derived from opsins have been extensively reviewed (6, 7) and are not discussed here.

In this review, we focus on flavoproteins and phytochromes as sources for molecular optical tools. We discuss the main classes of these photoreceptors, their chromophore binding domains, and light-induced chromophore transformations. We then overview genetically encoded tools based on photoreceptors and strategies for their design. Next, we focus on the engineering of FPs and biosensors. We discuss strategies to convert photoreceptors into permanently fluorescent FPs as well as to modify natural photocycles to yield photoactivatable FPs. We also consider fluorescent biosensors designed from photoreceptors. We overview and compare the properties of available fluorescent probes and discuss their applications, advantages, and limitations. We also consider recently developed OTs based on photoreceptors. We discuss principles of action for the different tools and describe their applications. For both optical probes and OTs, we focus on the systems with demonstrated applicability in mammalian cells or eukaryotic organisms.

NATURAL PHOTORECEPTORS AND THEIR MECHANISMS OF ACTION

LOV domains were found in plant phototropins (Figure 1) as well as in other photoreceptors in plants, bacteria, algae, and fungi with kinase, phosphodiesterase, DNA binding, and other functions (2, 4). They belong to the Per–Arnt–Sim (PAS) protein family. The small size (∼11–15 kDa) and presence of flavin chromophores in most, if not all, cell types are key advantages of these domains for the design of optical probes. Absorption of blue light by the FMN chromophore in LOV domains results in the formation of a thiol adduct between the C4a position of the isoalloxazine ring of FMN and conserved cysteine residue within the protein. In darkness, this reaction thermally goes in the reversible direction within 10 to 10^3 s. Signal propagation involves a side-chain rotation of the conserved flavin-interacting glutamine residue within the β-scaffold of the LOV core. Further signal transduction from the core to the C- or N-terminal extensions varies among LOV domains. In phototropins, signaling occurs through the undocking of a C-terminal Jα helix upon illumination.

BLUF domain–containing photoreceptors are important light sensors in bacteria and algae (8). They bind FAD as a chromophore. In contrast to an LOV domain, no covalent bond formation is involved in a BLUF photocycle. The primary chromophore transformations, which are sensed by neighboring amino acids and lead to signal propagation, are changes in the hydrogen-bond environment in the chromophore excited state and, possibly, electron-transfer reactions (2).

Cryptochromes (Figure 1) are found in all kingdoms of life (5). They regulate growth and development in plants and are involved in the regulation of the circadian clock in animals. Cryptochromes are closely related to photolyases and share a chromophore-binding photolyase homology region (PHR). In contrast to photolyases, cryptochromes incorporate only a single chromophore, FAD (9). Light induces an intramolecular redox reaction, which involves the FAD molecule and conserved tryptophan amino acid residues in a protein backbone, and results in cryptochrome structural changes and signal transmission.

Phytochromes are widespread photoreceptors found in plants, bacteria, cyanobacteria, and fungi, playing essential roles in light-adaptive processes (3, 10). They incorporate linear tetrapyrroles (bilins) as chromophores (Figure 1). Tetrapyrroles are the products of enzymatic degradation of a heme. In addition to phytochromes, two other groups of photoreceptors incorporate bilin chromophores: phycobiliproteins and cyanobacteriochromes (CBCRs).

Phycobiliproteins serve as antenna pigments involved in the photosynthetic apparatus of cyanobacteria and algae. These proteins are intensely fluorescent. However, their complex biochemical synthesis (cells need to produce an apoprotein, e.g., bilin reductases for chromophore synthesis and lyases for chromophore attachment) and large molecular mass (100–240 kDa) prevent their use as live cell probes.

Unlike phycobiliproteins, phytochromes and CBCRs incorporate bilin chromophores autocatalytically. Phytochromes share common domains in a photosensory core module (PCM), consisting of PAS, GAF (cGMP phosphodiesterase/adenylate cyclase/FhlA), and PHY (phytochrome-specific) domains. Bacterial and fungal phytochromes incorporate

tetrapyrrole, called biliverdin IXα (BV), as a chromophore. In plants and cyanobacteria, BV is enzymatically reduced to phytochromobilin (PΦB) and phycocyanobilin (PCB), which bind to plant and cyanobacterial phytochromes, respectively. The chromophore is covalently attached via the C3 side chain of the tetrapyrrole A-ring to a conserved cysteine in the PAS or GAF domain. Photocycle includes reversible photoisomerization of the bilin chromophore around its 15/16 double bond (Figure 1). This causes rotation of a D-ring and conformational changes in the protein backbone, which are transferred to an effector domain. The effector domain is typically represented by a histidine kinase. However, other effectors such as domains that interact with DNA repressors (11) and diguanylate cyclase and phosphodiesterase domains, involved in second messenger signaling (12), have been reported. CBCRs sense light in the entire visible spectrum owing to variations in the protein–bilin interactions, and their PCMs consist of several GAF domains. Interestingly, similar to CBCRs, phytochromes found recently in algae can sense blue, green, and orange light in addition to far-red and NIR light (13). All bilin-binding proteins absorb at 380–420 nm (the so-called Soret band), in addition to the main absorption peak (Q-band) specific to each phytochrome. Absorption at the Soret band corresponds to a single pyrrole ring of the bilin chromophore.

Among phytochromes, a subclass of bacterial phytochrome photoreceptors (BphPs) deserves special attention because they incorporate BV (14–16). BV has the most redshifted absorbance relative to other bilins (Figure 1), which lie in an NIR transparency window of mammalian tissues (650–900 nm). In contrast to other tetrapyrroles found in phytochromes, BV is readily available in mammalian tissues. Typically, the ground (inactive) state of BphPs is Pr (15/16 double bond in BV in *cis* conformation), which converts to the active Pfr state (15/16 double bond in *trans* conformation) upon illumination with 660–680-nm light. The Pfr state returns to Pr by slow dark (thermal) relaxation or fast 740–760-nm light-induced photoconversion. A specific group of phytochromes, termed bathy, adopt Pfr as a ground state.

Crystallographic studies of PCMs of plant phytochrome PhyB from *Arabidopsis thaliana* (17) and BphP *Dr*BphP from *Deinococcus radiodurans* (18) before and after illumination, as well as a structural analysis of bathy BphP *Rp*BphP1 from *Rhodopseudomonas palustris* (11), revealed a common mechanism for the conformational changes leading to phytochrome activation. Light-induced rotation of the chromophore D-ring causes rearrangement of hydrogen bonds in a chromophore binding pocket. As a result, the evolutionarily conserved part, called the tongue, of the PHY domain that extends to the bilin binding pocket and forms a distinctive hairpin structure undergoes refolding. In the Pr state, the main part of the tongue consists of two β-sheets, whereas in the Pfr state it converts into an α-helix. Changes in the tongue structure result in conformational changes to the effector domain that lead to enzyme activation or exposure of the sites interacting with the protein partners.

FLUORESCENT PROTEINS ENGINEERED FROM PHOTORECEPTORS

Photoreceptors as Templates for Engineering of Fluorescent Proteins

Green fluorescent protein (GFP) and related FPs have been widely applied in diverse areas of research (19). However, there are applications in which the performance of the GFP-like proteins is poor or no GFP-like FPs with required properties are available. The limitations of GFP-like proteins include (*a*) dependence of chromophore formation on molecular oxygen, (*b*) relatively large size (~27 kDa), and (*c*) limitation of their absorbance and fluorescence to a visible part of the spectrum. Photoreceptors serve as templates to engineer FPs with properties, which cannot be developed in GFP-like FPs.

For the design of fluorescent probes, the nature of the chromophore is essential. It defines the range of wavelengths of absorbed and emitted light, the properties of the FPs, and the requirements for their applications. Eukaryotic cells naturally produce FMN and BV chromophores. If these chromophores bind to the engineered FPs efficiently, then applications of this FP require delivery of only a single gene encoding the FP, similar to GFP-like FPs. In other cases, chromophores should be exogenously supplied or additional genes for chromophore synthesis should be incorporated into the cells. The general strategy to design permanently fluorescent FP from photoreceptors is to block the photocycle to transform the energy of excitation light into fluorescence emission. However, some FPs retain their photoswitching properties for a new functionality.

Fluorescent Proteins Developed from LOV Domains

Two properties of LOV domains, their small size (~10–15 kDa) and their independence of molecular oxygen, justified their use for FP engineering. To create a permanently fluorescent LOV-based FP, one can abolish its photocycle by mutating the key photoactive cysteine in the active site (20). Subsequent random mutagenesis allowed for the improvement of brightness and photostability (Figure 2a).

Early LOV-based FPs (so-called FbFPs) were developed from bacterial blue-light photoreceptors *Pseudomonas putida* SB2 and *Bacillus subtilis* YtvA (Table 1) (21). Interestingly, both SB2 and truncated YtvA, consisting of an LOV domain only, are dimers, whereas full-length YtvA with a C-terminal effector domain is a monomer. Two FPs were obtained from YtvA, such as *Bs*FbFP, which is the full-length YtvA/Cys26Ala, and *Ec*FbFP, which is the YtvA/Cys26Ala truncated to the LOV domain. The fluorescent BS2/Cys53Ala mutant was termed PpFbFP. Engineered FbFPs were successfully applied as reporters in bacteria growing under normal and anaerobic conditions and in mammalian cells (21, 22). Two other LOV domains were converted to LOV-based FPs via substitution of a conservative cysteine to alanine, thus yielding *Ds*FbFP from *Dinoroseobacter shibae* and *Pp*1FbFP from *Pseudomonas putida* (23). However, similar to other bacterial LOV domains, these proteins are dimeric; they also do not possess characteristics superior to those of FbFPs.

iLOV is a photoreversible FP engineered from the LOV2 domain of the *A. thaliana* phot2 phototropin (*At*phot2) (24). It was obtained by introducing a key cysteine-to-alanine substitution followed by gene shuffling using LOV domains of two phototropins, *At*phot1

and *At*phot2. In contrast to bacterial LOV-based FPs, iLOV is monomeric and localizes correctly in fusion constructs in plant cells. Owing to its small size, iLOV performed better than GFP as a reporter for viral movement in plants (24). Thus, iLOV is a good choice for applications in which steric constraints may impact protein translocation or if reduced genetic load in labeled virus is required (Table 1) (Figure 2b).

Original iLOV displayed low photostability and reversible photobleaching (spontaneous recovery with a half-time of ∼50 s). These characteristics likely reflect a reversible photochemical transformation of FMN under high light intensities, such as the formation of nonfluorescent neutral semiquinone species. Structural studies combined with directed molecular evolution allowed researchers to engineer a photostable derivative of iLOV, termed phiLOV 2.1 (25).

A different property of FMN-containing LOV domains became crucial for the design and application of LOV-based FP, termed miniSOG (mini singlet oxygen generator) (26). Shu et al. (26) utilized the known fact that FMN efficiently generates singlet oxygen species (Figure 2b). If FMN retains the ability to generate reactive oxygen species (ROS) within a protein, such proteins can direct the ROS generator to a specific location in a cell. To obtain miniSOG, libraries of mutants obtained using LOV2 domains of *At*phot2 were screened for efficient photodestruction of a fused BphP-derived IFP1.4 protein. Interestingly, recent studies demonstrated that a quantum yield of singlet oxygen production by miniSOG is relatively low (0.03) compared with that of free FMN (0.51) (27). However, prolonged irradiation increases quantum yield significantly, probably via photoinduced FMN transformations in a protein. Overall, miniSOG shares four key amino acid substitutions with iLOV, including a mutation of a key cysteine to glycine. An additional mutation N390S is shared with phyLOV2.1, which may provide FMN stabilization and is responsible for improved photostability (25). Monomeric miniSOG was tested for correct localization in various fusions in mammalian cells.

MiniSOG allowed for correlative light and electron microscopy applications, including imaging of synaptic cell adhesion molecules in mouse brain tissues (26). In fixed tissue, generated singlet oxygen locally polymerizes added diaminobenzene into a precipitate, which can be stained with osmium and imaged at a resolution of tens of nanometers.

An ability to generate ROS turns an FP into an OT, such as a photosensitizer. When fused to a protein, miniSOG induces chromophore-assisted light inactivation that inactivates a protein molecule (28) or kills a whole cell when targeted to mitochondria (29) or plasma membrane or fused with the DNA-binding protein H2B (30). Although miniSOG is functional in cultures of tumor cells and in transparent animals such as *Caenorhabditis elegans*, no substantial photodamage was observed in a tumor xenograft expressing miniSOG in mice (30). This can result from the low penetration of blue light in mammalian tissues and reduced levels of FMN in tumors. The photosensitizer properties of miniSOG are likely not unique and are possibly exhibited by other LOV-based FPs.

LOV-based FPs with an unblocked photocycle have also been explored. Wild-type YtvA has a weak fluorescence and can be photoswitched between the fluorescent and dark states using

continuously running, weak 405-nm activation and 488-nm readout lasers. This property was utilized in imaging of *Escherichia coli* with super-resolution photoactivated localization microscopy (31).

Fluorescent Proteins Engineered from Phytochromes

The main advantage of using phytochromes as templates for FPs is that they can be engineered into redshifted FPs for noninvasive imaging and readout in animals. BphPs, in particular, incorporate the most redshifted BV chromophore and have become a widely explored source for the design of NIR FPs (Figure 2). BV is ubiquitous in mammalian tissues, in contrast to PCB and PΦB. In the NIR transparency window, mammalian tissue is most transparent to light because the combined absorbance of hemoglobin, melanin, and water is minimal (32).

To engineer FP from a phytochrome, its photoswitching should be blocked by stabilizing the Pr state and disrupting a hydrogen-bond network between the chromophore and the protein backbone, leading to nonradiative dissipation of energy (33, 34). This can be achieved by preventing light-induced chromophore isomerization or by incorporating heterologous chromophores, which cannot isomerize. The latter approach was demonstrated by substituting PCB with phycoerythrobilin (PEB), which has saturated bonds between the C- and D-rings (35). As a result, FPs with quantum yield of up to 0.72 from the cyanobacterial phytochrome Cph1 and 0.55 for CBCRs were obtained. However, these FPs fluoresce in the orange part of the spectrum and require a PEB supply.

In phytochromes, the PAS and GAF domains are minimally required to covalently attach a bilin chromophore, whereas the PHY domain participates in chromophore photoconversion and signal transduction (36). Thus, the PAS and GAF domains serve as templates for permanently fluorescent NIR FPs, whereas the PAS, GAF, and PHY domains are required to engineer photoswitchable NIR FPs (Figure 2c). Natural phytochromes are dimers with the α-helices of the GAF and PHY domains forming a dimeric interface (33). FPs engineered from BphPs can be monomerized by disrupting this interface. However, for the purposes of labeling whole cells and organelles, monomerization is not required.

Early studies revealed amino acid substitutions that render phytochromes fluorescent (37). A single mutation in the GAF domain, Y176H, was sufficient to make the PCMs of Cph1 (37) and plant phytochrome *At*PhyB (38) fluorescent. A combination of a similar mutation, Y263F, and a mutation in the conserved PASDIP amino acid motif, D207H, yielded an FP called Wi-Phy from the monomerized PAS and GAF domains of *Dr*BphP (33).

The first BphP-derived FP with demonstrated use in mammalian cells and in mouse liver is IFP1.4 (Table 1) (39). It was engineered from the PAS and GAF domains of *Dr*BphP by introducing a D207H mutation and mutagenesis of residues near the D-ring to prevent nonradiative energy dissipation. In in vitro assays, IFP1.4 is monomeric; however, its intracellular localization in critical fusions was not tested. Other limitations of IFP1.4 include its dependence on the supply of exogenous BV and low effective brightness in mammalian cells.

An improved version of IFP1.4, IFP2.0, also requires the BV supply (40). However, in the excess of BV, its brightness increases severalfold. IFP2.0 was utilized to label cells engineered to coexpress a heme oxygenase, HO-1, for intracellular production of BV. The IFP1.4 mutagenesis, which led to IFP2.0, also resulted in its dimerization and in the formation of protein species in the IFP2.0 population having blueshifted excitation and emission. IFP2.0 plus the HO-1 system has allowed researchers to noninvasively image neurons in *Drosophila* larvae and brain tumors in mice. HO-1 coexpression mitigated variations in the BV level in different cell types and provides its large excess for efficient incorporation in BphP-based FPs. However, this approach may affect cell metabolism and proliferation because heme oxygenase is a stress response enzyme.

As the field of engineering NIR FPs has developed, it has become clear that in addition to molecular brightness (a product of extinction coefficient and quantum yield) and photostability, effective cellular brightness should be considered (Table 1). Cellular brightness of BphP-derived FPs depends on molecular brightness, intracellular folding and stability, affinity and specificity to the BV chromophore, intracellular BV concentration, and protein expression level. Low efficiency and specificity of BV binding substantially decrease cellular fluorescence. Other heme-related compounds such as protoporphyrin IX may compete for binding to the BphP apoprotein (41).

The first NIR FP specifically optimized for high brightness in mammalian cells without exogenous BV was iRFP (later renamed iRFP713) (42). iRFP713 was engineered from the PAS and GAF domains of *Rp*BphP2. Efficient and specific binding of BV in iRFP713 was the result of extensive screening of mutants for fluorescence in mammalian cells. High efficiency of BV incorporation allowed the use of iRFP713 simply by transfecting a single gene into cells.

Subsequently, four spectrally distinct NIR FPs, iRFP670, iRFP682, iRFP702, and iRFP720, which have properties similar to those of iRFP713, were engineered (43). iRFPs were developed from the PAS and GAF domains of *Rp*BphP2 and *Rp*BphP6 by applying molecular evolution directed toward spectral shifts. Similar to iRFP713, these proteins are dimers. Spectrally distinct iRFPs enabled labeling of two and more mammalian tissues for tracking cell populations noninvasively in an animal (Figure 2d). Although iRFPs do not require exogenous BV to fluoresce in many eukaryotic cells and organs of mammals, its supply may be helpful for cell types with very low endogenous BV levels. Another situation when iRFPs may work inefficiently is when they do not tolerate fusions with particular proteins. iRFPs are advantageous for in vivo imaging (Figure 2d). This has been demonstrated in direct comparison with far-red GFP-like FPs (43). NIR FPs, including iRFPs, have already been applied to a variety of applications in neuroscience, stem cell biology, developmental biology, and cancer research (44–46). High extinction coefficients enabled their use beyond fluorescence imaging as deep-tissue probes for photoacoustic tomography (47).

Engineering of phytochrome-derived FPs, which undergo a reversible photoswitching between two states, has also been explored. This resulted in an FP developed from the GAF3

domain of a PCB-binding CBCR, which was called RGS and photoconverted between green and red states (48).

Two photoactivatable NIR FPs based on a PCM of *At*BphP from *Agrobacterium tumefaciens* C58 have been engineered (49). Rational and random mutagenesis was applied to stabilize the Pr state and enhance its fluorescence in *At*BphP-derived variants with Pfr–Pr photoconversion. Two obtained proteins, PAiRFP1 and PAiRFP2, can be photoactivated by a wide range of far-red and NIR light with larger power (>2 mW/cm^2 at 650 nm) than is used for in vivo imaging (~6 $\mu W/cm^2$ at 650 nm). In PAiRFPs, the Pr–Pfr photoconversion is disabled, whereas the kinetics of dark reversion from the Pr state back to the Pfr state is considerably extended (Table 1). An important application of PAiRFPs is deep-tissue in vivo imaging under highly autofluorescent conditions. The high signal-to-background ratio is achieved by subtracting the images made before and after photoactivation. PAiRFPs can also be applied for photolabeling and short-term noninvasive tracking in animals.

FLUORESCENT SENSORS BASED ON PHOTORECEPTORS

Biosensors Derived from LOV Domains

Genetically encoded biosensors and reporters based on GFP-like FPs have enabled researchers to monitor changes in the intracellular environment, such as variations in concentrations of different ions and cellular metabolites, protein–protein interactions (PPIs), and enzymatic activities (19). Specific properties of FPs developed from photoreceptors can be utilized to engineer sensors with unique characteristics that are inaccessible with GFP-like reporters. Independence of fluorescence of LOV-based FPs on molecular oxygen was utilized to design the first genetically encoded FP-based biosensor for oxygen (FluBO) (50). FluBO is a FRET (Förster resonance energy transfer) sensor consisting of cyan fluorescent hypoxia-tolerant *Ec*FbFP as a donor and oxygen-sensitive yellow fluorescent protein (YFP) as an acceptor (Figure 3a). In aerobic conditions, both proteins form chromophores and efficient FRET occurs. In the absence of oxygen, the YFP chromophore does not mature and FRET coupling is lost. FluBO performance was validated in bacteria. However, because oxygen-dependent chromophore formation is irreversible, FRET changes reflect not only the decrease of oxygen concentration but also the stability of the reporter and its intracellular turnover. The response kinetics to increasing oxygen concentrations depended on the time needed for reporter synthesis and YFP chromophore formation. It remains to be tested if a FluBO performance can be improved by fusing the weak degradation motif for its fast turnover.

Reporters Engineered from Phytochromes

NIR fluorescence of BphP-derived FPs justifies their choice as templates for biosensors and reporters for in vivo studies. Specific properties of a bound BV chromophore can also be utilized. There are two types of BphP-derived reporters: IFP1.4 as a sensor for ions and reporters for PPI based on a bimolecular fluorescence complementation (Table 2).

The ability of Hg^{2+} ions to block a conserved cysteine in the PAS domain from binding to BV was explored to detect these ions in vitro and in cells (51). In the presence of Hg^{2+}, IFP1.4 did not incorporate BV and did not develop fluorescence. The dependence of IFP1.4

on endogenously added BV turned out to be an advantage for the Hg^{2+} assay in mammalian cells, because binding reactions of both BV and Hg^{2+} are irreversible and notable fluorescence before addition of BV may prevent Hg^{2+} detection. However, the sensitivity of mercury detection in cells appeared to be rather low: A fivefold fluorescence decrease was observed in cells with 32 μM Hg^{2+} compared with 50 nM in vitro. Free intracellular thiols may have competed for binding to Hg^{2+}.

The domain organization of BphPs provided the possibility of designing split PPI reporters on the basis of molecular complementation of the PAS and GAF domains into an FP molecule (Figure 3b). A natural linker between these domains is a preferable location for polypeptide breakage. However, a figure-eight knot between an N-terminal extension of the PAS domain and a loop of the GAF domain in BphPs may affect complementation efficiency and reversibility.

The first NIR PPI reporter, named iSplit, was engineered from the PAS and GAF domains of iRFP713 (52). To develop a bright reporter with a high complementation contrast (up to 50-fold), the GAF domain was subjected to directed molecular evolution. Similar to iRFP713, reconstituted iSplit efficiently incorporated endogenous BV and did not require its exogenous supply. iSplit was utilized as a PPI reporter in cultured mammalian cells and in tumors in mice. Although the reporter is irreversible, detection of repetitive binding events was possible because iSplit intracellular stability is lower than that of iRFP713.

Another split BphP-based reporter, IFP PCA (infrared fluorescent protein–protein fragment complementation assay), was derived from IFP1.4 (53). Similar to iSplit, two parts of IFP PCA included the PAS and GAF domains. IFP PCA was 10-fold less bright than iSplit and required a supply of the large excess of exogenous BV. It also suffered from low contrast in mammalian cells. However, unlike iSplit and complementation systems developed on GFP-like FPs, IFP PCA is reversible. The reconstituted fluorescent reporter unfolded upon dissociation of interacting protein partners with kinetics similar to that observed in other studies of the same PPIs. Reversibility has allowed spatiotemporal localization of PPIs in yeast and mammalian cells.

The apparent reversibility of IFP PCA raises a question about its origin. A figure-eight knot between the PAS and GAF domains should prevent dissociation of split fragments. Also, BV in a chromophore binding pocket of the GAF domain is covalently linked to the cysteine at the N terminus of PAS domain. It was demonstrated that covalently bound BV tightens the knot and prevents renaturation of unfolded protein (54). A possible explanation for IFP PCA reversibility is the presence of a substantial fraction of reconstituted IFP1.4 with noncovalently incorporated BV. Another possibility is that the reversibility is caused by the fast intracellular degradation and turnover of the reporter.

OPTOGENETIC TOOLS DERIVED FROM PHOTORECEPTORS

Design Principles and Practical Requirements for Optogenetic Tools

Owing to the natural ability of photoreceptors to sense light by the PCM and convert it into a meaningful intracellular signal in the effector domain, they have been widely used as

templates for the engineering of OTs. OTs have been created using several approaches to trigger biological responses. These approaches include activation of desired intracellular processes by photoinduced deactivation of steric inhibition; activation of the synthesis of second messengers; and induction of PPIs such as homodimerization, oligomerization, or heterodimerization (Figure 4).

Successful application of OTs depends on several of their characteristics. OTs must be readily expressible in the target organism or tissue and have the correct folding and localization. To achieve the desired level of expression, the use of appropriate promoters may be necessary. The sizes of fusion OTs expressed are also important to consider. The smaller size of the PCM allows for fusion of the larger effector part without affecting intracellular localization and functionality of the fusion. Another important property is the ability to specifically and efficiently utilize the endogenous chromophore and to incorporate it autocatalytically. Ideally, OTs should be orthogonal, meaning they should minimally interfere with the endogenous metabolism. Other essential requirements for OTs are low background activity, fast kinetics of activation, large dynamic range, high sensitivity to activation light, and the ability to undergo a large number of activation–deactivation cycles. Moreover, a narrow spectral range of light sensitivity is highly desirable for an OT to be coexpressed with additional tools or FPs with spectrally distinct properties. The possibility of switching an OT off using light, or at least its fast thermal relaxation back to the ground state, provides an advantage for precise spatiotemporal control.

The ultimate goal of applying OTs in living animals imposes additional requirements, such as low cytotoxicity and a sufficient level of expression that does not interfere with normal physiological functions. Low phototoxicity of activation light is essential, too. The latter requirement limits applications of OTs, which utilize blue light for activation. OTs for in vivo applications should be controlled by NIR light, which penetrates deeply in mammalian tissues, allowing for noninvasive control of physiological processes in the desired organs of model animals.

Optogenetic Constructs Designed from LOV Domains

Among photoreceptors, small and well-studied LOV domains are most widely utilized as templates to engineer OTs. The two main strategies for designing OTs differ in their mechanisms. The first strategy is based on a structural change in a single LOV domain, resulting in the uncaging of an active protein interface (Figure 4a). For this purpose, a monomeric asLOV2 domain derived from phototropin 1 of *Avena sativa* (*As*phot1) is frequently used. Illumination with blue light leads to unwinding of the docked (caged) Jα helix and exposure of the fused C-terminal peptide epitope or protein interface, thus making them available for enzymatic activity or PPI. In wild-type LOV domains, equilibrium is found between docked and undocked conformations in both dark and light states. Site-directed mutagenesis of an interaction interface between the Jα helix and LOV core can affect this equilibrium and substantially decreases undesirable Jα helix uncaging in the dark state, consequently increasing the dynamic range (55–57). Knowledge-based structure modifications can also enhance the light sensitivities of OTs (55, 58, 59).

The second strategy to develop LOV-derived OTs is based on light-induced homodimerization or heterodimerization of photoreceptors containing LOV domains (Figure 4c,d). The homodimerization approach utilizes one of the smallest LOV domain–containing proteins, called Vivid (VVD) from *Neurospora crassa*. Compared with asLOV2, VVD lacks the C-terminal Jα helix but has an N-terminal helix (Ncap) that is docked on the core in the dark state. In contrast to other LOV domains, VVD binds FAD chromophore. Illumination leads to the dissociation of Ncap from the VVD core and interaction with Ncap of another VVD, resulting in a VVD dimer (60, 61). The heterodimerization approach employs an interaction between the LOV-containing flavin-binding kelch repeat F-box 1 (FKF1) protein with its natural partner, GIGANTEA (GI). Illumination induces FMN to bind with FKF1, which allows FKF1 to interact with GI. The cysteinyl–flavin bond is subsequently hydrolyzed, returning the LOV domain to its dark state and causing dissociation of the FKF1–GI heterodimer (62).

The first LOV-based OT was engineered using a caging strategy (Figure 4a). The engineered fusion between asLOV2 and small GTPase Rac1 effectively controlled the actin-based cellular contractility and movement of mammalian cells (63). In the caging principle implemented in the tool, Rac1 effector binding was sterically blocked by fusing an asLOV2 domain to the N terminus of Rac1. Illumination with 458-nm light caused Jα helix unfolding and dissociation of the asLOV2 core from Rac1, and this change in the tertiary structure of the fusion removed the inhibition (Figure 5a). The system possessed full reversibility in darkness. The similar effective caging of the enzyme and inhibition of activity were also shown for caspase-7 (64). The truncated catalytic domain of caspase-7 was fused to the C terminus of the Jα helix of asLOV2. Blue-light stimulation of the fusion resulted in apoptosis.

Application of the steric inhibition approach was expanded to caging of small effector peptide epitopes on the core of asLOV2. A vinculin-binding peptide, ipaA, was caged on the asLOV2 core by enhancing the Jα helix–peptide interaction interface with the core via point mutations (65). Then the LOV2–ipaA fusion was applied to the transcription activation of a gene under control of the Gal4 promoter. A similar approach resulted in a LovTAP OT that allowed blue-light control of the interaction of the tryptophan repressor (TrpR) with DNA (56). For this, the tryptophan repressor TrpR should form an active dimer. Strickland et al. (56) caged 11 N-terminal residues of TrpR, important for the formation of the dimer, with the Jα helix of asLOV2 such that TrpR dimerization was sterically blocked. Illumination with 470-nm light caused Jα unwinding and formation of TrpR dimers able to bind their cognate DNA sequence.

Further development of the caging strategy led to the creation of an OT based on an interaction between the asLOV2 and ePDZ domains, called tunable light-induced dimerization tags (TULIPs) (66). Strickland and colleagues (66) fused a peptide epitope, which is recognized by ePDZ, to the C terminus of the Jα helix and applied site-directed mutagenesis to cage the resulting chimeric helix on the asLOV2 core. Illumination with 473-nm light led to the recruitment of ePDZ to membrane-anchored asLOV2, as demonstrated in mammalian and yeast cells. This approach was applied to arrest the cell cycle by initiating a MAPK cascade and to Cdc42-mediated control of cell polarity (Figure 5b).

Light control of PPIs can be implemented through the homodimerization strategy (Figure 4d). This approach was used to develop a so-called LightON system based on VVD, which homodimerizes in blue light (67). VVD was fused with the Gal4 DNA-binding domain and the p65 transcription activation domain. After using mutagenesis to reduce the VVD dark-state background dimerization, the LightON system was applied to regulate transgene expression. A 200-fold increase in expression of mCherry from the galactose-responsive promoter was observed after stimulation with 460-nm light. Dark relaxation to the not-activated state occurred with a half-time of 2 h. Light-driven expression was controlled by the number and length of the blue-light pulses. LightON was also applied to express Cre recombinase and insulin in mice. Advantages of the LightON system are that it is small in size, has high sensitivity to light, and has a large dynamic range.

The homodimerization strategy was also used to design OTs for gene expression based on the LOV domain–containing photoreceptor EL222 from *Erythrobacter litoralis* (68). EL222 consists of an LOV domain and an HTH (helix-turn-helix) domain. Blue-light illumination leads to dissociation of the HTH domain, caged in darkness on the EL222 photosensory core, and subsequent EL222 dimerization through the LOV and HTH interfaces (69). To activate transcription in mammalian cells, a VP16 activation domain was fused to the N terminus of EL222. This OT produced up to a 100-fold increase in luciferase expression in cells and provided mCherry expression in zebrafish embryos. In comparison with the LightON system, the EL222-based construct has more rapid activation (10 s) and deactivation (50 s) kinetics and a linear response to light. However, both systems have specificity to only a single cognate DNA sequence. Recently, seven various LOV domains were compared as templates for engineering light-activated FGFR (fibroblast growth factor receptor). Grusch et al. (70) found that the LOV domain of aureochrome 1 from *Vaucheria frigida* was the most effective for blue-light-driven homodimerization of the FGFR intracellular domain.

The heterodimerization strategy (Figure 4c) was applied to develop a blue-light-responsive tool based on an inducible interaction between FKF1 and GI from *A. thaliana* (71). Yazawa and colleagues (71) fused FKF1 with the cytoplasmic variant of GTPase-null Rac1 and anchored GI to the plasma membrane via the CAAX targeting peptide. Illumination with 450-nm light caused relocalization of the FKF1–Rac1 fusion to the plasma membrane and subsequent lamellipodia formation with micrometer spatial precision (Figure 5c). The GI and FKF1 interaction was also utilized to develop the LAD (light-activated dimerization) system, in which GI and FKF1 were fused with the Gal4 DNA-binding and VP16 transcription activation domains, respectively (Figure 5d). Blue-light stimulation of cells expressing LAD resulted in a fivefold increase of the transcription level from the galactose-responsive promoter.

An alternative transcription activation OT, based on the GI and FKF1 interaction, utilized a zinc-finger protein (ZFP) instead of the Gal4 DNA-binding domain (72). This system, called LITEZ (light-inducible transcription using engineered zinc-finger proteins) provided a 53-fold increase in reporter gene transcription in mammalian cells after illumination with 450-nm light. The reporter gene was controlled by minimal promoter with nine repeats upstream of the ZFP-binding motif (Figure 5d). The system was tunable using both light intensity and

the number of ZFP motif repeats, and it was fully reversible to the basal level after 24 h in darkness. A notable drawback of the LAD and LITEZ constructs is the larger size of the involved proteins as compared with those used with VVD tools. The major characteristics of the OTs based on LOV domains and a comparison between them are summarized in Table 3.

Optogenetic Tools Engineered from BLUF Domains and Cryptochromes

Similarly to LOV domain–containing photoreceptors, BLUF domains and cryptochromes sense light in the blue region of the spectrum. However, to do so, they utilize the FAD chromophore exclusively. A typical mechanism of action of BLUF-based OTs is light-induced BLUF structure changes, resulting in activation of the inhibited in a dark-state enzymatic activity (Figure 4b). The first system to utilize this approach, called euPAC, was composed of two α-subunits (PACα) or two β-subunits (PACβ) of photoactivated adenylyl cyclase from *Euglena gracilis* (73). Each subunit harbors two BLUF-type photoreceptor domains and two catalytic domains. In darkness, the cAMP level in *Xenopus* oocytes injected with euPACα mRNA was already 20-fold higher than in noninjected oocytes, revealing substantial leakage of the euPAC system. Illumination with blue light resulted in a 10-fold cAMP increase over nonilluminated injected oocytes. In vivo application of euPACα was demonstrated in *Drosophila* brain when stimulation with 455-nm light led to behavioral changes related to the cAMP cellular level. These alterations were fully reversible after turning the light off. Later, such drawbacks of the euPAC system, such as large size of the involved proteins and high background, were overcome by utilizing adenylyl cyclase from *Beggiatoa* proteobacteria. Called bPAC (74), this tool contained only a single BLUF domain and a single catalytic domain, which resulted in its substantially smaller size (40 kDa instead of 110 kDa of euPAC). Injection of bPAC's mRNA into *Xenopus* oocytes followed by stimulation with 455-nm light caused a 300-fold increase of the cAMP level. bPAC coexpressed with cAMP-dependent ion channels in *Drosophila* neurons showed light-inducible behavioral changes in flies. bPAC was activated more slowly and inactivated much more slowly than was euPAC. Owing to the long lifetime of the bPAC active state, its half-saturating light intensity is low, and bPAC requires ∼1,000-fold-lower light intensity than euPAC to achieve the same cAMP level. The bPAC system demonstrates effective regulation of cellular processes by a natural photoreceptor. Further development of this system resulted in the design of the photoactivated guanylyl cyclase BlgC (75).

Cryptochromes, similarly to BLUF domains, incorporate the FAD chromophore. Many OTs are based on *A. thaliana* cryptochrome 2 (CRY2). This protein undergoes a blue-light-induced homo-oligomerization, which may lead to activation of a protein of interest fused to CRY2 (Figure 4d). CRY2 also participates in light-stimulated heterodimerization with its natural partner CIB1 (CRY-interacting bHLH1). In this approach, it is possible to regulate PPIs by controlling their subcellular localization (Figure 4c).

Recently, an OT based on CRY2 homo-oligomerization was developed to control gene expression and cell morphology (76). The N-terminal PHR domain of CRY2 was fused with the C-terminal domain of LRP6 (LRP6c), which activates a β-catenin pathway when

dimerized. Stimulation of CRY2–LRP6c transfected cells carrying a β-catenin-responsive luciferase reporter with 488-nm light increased the level of β-catenin activity up to ∼200-fold. The homo-oligomerization approach was also applied for activation of RhoA. In this case, illumination of mammalian cells carrying CRY2–RhoA fusion caused its translocation from the cytoplasm to the membrane and was accompanied by cell spreading. Both processes were reversible on a minute timescale in darkness. In a similar approach, blue-light-dependent dimerization of CRY2 was utilized to active C-RAF, an upstream member of the RAF/MEK/ERK pathway (77). Though both the homo-oligomerization of CRY2 and the hetero-oligomerization of CRY2–CIBN were studied (Figure 5e), the former process showed more effective light activation.

CRY2 homo-oligomerization was also implicated in an opto-FGFR1 tool consisting of the cytoplasmic region of FGFR fused with CRY2 (78). Typically, FGFR dimerization causes its cytoplasmic regions to *trans*-autophosphorylate multiple tyrosine residues, thereby providing docking sites for downstream pathway components. Therefore, the cytoplasmic region of FGFR was fused with the PHR domain of CRY2. Cotransfection of opto-FGFR1 and biosensors for distinct FGFR canonical pathways showed light-induced activation of PLCγ, MAPK, and PI3K pathways with spatiotemporal resolution. The activation was fine-tuned by the light frequency and duty cycle of photostimulation. Full reversibility of the system was observed 1 h after turning off the light for the ERK1 pathway. Opto-FGFR1 allowed light-induced regulation of cell polarity and migration of endothelial cells through the PI3K and PLCγ pathways. Cell morphology light control was also obtained using a heterodimerization approach, in which CRY2 fused with the inositol 5-phosphatase domain of OCRL (5-ptase$_{OCRL}$) interacts with membrane-anchored CIBN (79). Illumination of cells resulted in the relocalization of CRY2–5-ptase$_{OCRL}$ to the plasma membrane, where it caused the rapid (within seconds) and reversible (within minutes) dephosphorylation of its targets.

Formation of large clusters was utilized to inhibit the protein of interest in an OT, LARIAT (light-activated reversible inhibition by assembled trap), in which CRY2 homo-oligomerization is coupled with its heterodimerization with CIB1 (80). Clustering was further enhanced by fusing CIB1 with the naturally oligomerizing C-terminal region of CaMKIIα, called the MP (multimeric protein) (Figure 5g). Stimulation with 458-nm light of cells cotransfected with a fusion of CRY2 and Vav2, which is a guanine nucleotide exchange factor activating Rho small GTPases, and CIB1–MP led to trapping of CRY2–Vav2 in clusters followed by rapid retraction of lamellipodia, in which the activity of Rac1, a downstream target of Vav2, was partially attenuated. This approach was extended by fusing CRY2 with anti-GFP nanobody and tagged Rac1, Tiam1, Vav2, RhoG, and Cdc42 with GFP. In all cases, the GFP-tagged protein was inactivated in a light-dependent manner, thus controlling cell morphology. An advantage of the LARIAT system is that it potentially inhibits any GFP-tagged protein by surrounding it with a large cluster, whereas a significant drawback of this system is the extensive cluster formation that can cause cytotoxicity.

CRY2–CIB1 heterodimerization was also utilized to engineer light-inducible transcriptional effectors, called LITEs (81). The developed OT is based on DNA-binding domains from *Xanthomonas* sp., called TALEs (transcription activator–like effectors), which are

customizable for binding to DNA sequences of interest. Use of the PHR domain of CRY2 fused with a TALE and the CIB1 partner fused with the transcription activator VP64 resulted in the upregulation of *Neurog2* mRNA as early as 30 min after light stimulation. Application of the *Grm2*-targeted LITE construct in primary cortical neurons and in mouse brain resulted in seven- and twofold increases, respectively, in *Grm2* mRNA levels. The histone acetylation level was also light modulated in Neuro2a cells and in primary neurons, thus demonstrating possible epigenetic applications of LITE OTs. Overall, the OTs developed from CRY2 have more versatile applications than do LOV domain systems (Table 3). Compared with FKF1–GI, the CRY2–CIB1 pair has a smaller size. Moreover, the use of CRY2 allows researchers to combine the homo-oligomerization of CRY2 molecules with the subsequent hetero-oligomerization with CIB1.

Optogenetic Constructs Derived from Phytochromes

One of the major advantages of phytochromes over other natural photoreceptors used to engineer OTs is their sensitivity to NIR light, which is nonphototoxic for live cells. Different BphPs and plant phytochromes have been explored to design OTs that are applicable to mammalian cells and eukaryotes. The first BphP-based OT applied in the eukaryotic organism was developed using BphG1 from *Rhodobacter sphaeroides* (82). Unlike most BphPs, noncanonical BphP BphG1 has the GGDEF and EAL C-terminal domains, which control the turnover of c-di-GMP in bacteria. To create a meaningful biochemical signal for eukaryotic cells, the PCM of BphG1 was fused with the adenylate cyclase domain from the *Nostoc* sp. CyaB1 protein, followed by additional mutagenesis of the fusion. The chimeric BphG–CyaB1 protein was called an infrared-light-activated adenylate cyclase (IlaC) (Figure 6a). Activation of purified IlaC with 700-nm light resulted in a sixfold increase in cAMP levels. When expressed in cholinergic neurons of *C. elegans*, IlaC caused increased locomotion of the worms under NIR light, as the elevated intracellular cAMP upregulated acetylcholine release and led to subsequent activation of downstream muscle cells (83).

Another NIR OT, called a light-activated phosphodiesterase (LAPD), was designed on the basis of the canonical BphP *Dr*BphP (84). The PCM of *Dr*BphP (18) was fused with a catalytic domain of human phosphodiesterase 2A (85), which possesses cAMP- and cGMP-specific phosphodiesterase activities (Figure 6b). Illumination of the purified LAPD with 690-nm light caused a sixfold increase in the cGMP hydrolysis rate and a fourfold increase in the cAMP hydrolysis rate. LAPD was applied to modulate the intracellular levels of cyclic nucleotides in mammalian cells and zebrafish embryos. A notable decrease of cGMP was observed in cultured cells and up to a 40% decrease of cAMP in zebrafish embryos upon illumination with NIR light of the low 1.1 mW/cm^2 intensity.

Unlike OTs designed from BphPs, which utilize the enzyme activation approach (Figure 4b), OTs developed from plant phytochromes exploit light-induced heterodimerization (Figure 4c). The first OTs based on the plant phytochromes PhyA and PhyB from *A. thaliana* utilized a light-induced PPI with phytochrome-interacting factor 3 (PIF3). PIF3 is a basic helix-loop-helix protein, which interacts specifically with the Pfr form of both PhyA and PhyB (86, 87). This interaction was exploited to develop a light-switchable gene expression system based on the yeast two-hybrid concept. PIF3 was fused with an activation

domain of Gal4 (GAD), and the full-length PhyA or PCM of PhyB was fused to a DNA-binding domain of Gal4 (GBD). NIR light supported the growth of yeast colonies cotransformed with PIF3–GAD and PhyA–GBD or PhyB–GBD on a selective medium containing the added PCB chromophore. PhyB–GBD and PIF3–GAD interactions activated by single pulses of NIR light gave a 1,000-fold increase in the β-galactosidase assay above background (88). The PhyB–PIF3 interaction was reversible, and dissociation could be activated with 748-nm light.

Optimization of the binding of phytochrome-interacting factor 6 (PIF6) to PhyB resulted in the development of an OT that allowed light-controllable recruitment of a protein of interest fused with PIF6 to PhyB anchored to the plasma membrane (Figure 6c) (89). This interaction was reversible. Translocation could be induced with 650-nm light, which switches the Pr state into the Pfr state, and was terminated with 750-nm light. The fast forward and reverse kinetics of the PhyB–PIF6 interaction made possible the fine spatiotemporal control of activity of the Rho family GTPases fused with PIF6 in mammalian cells (89).

PhyB–PIF6 heterodimerization was also utilized to control gene expression in mammalian cells (90). For this, a concept of the split transcription factors was applied. The tetracycline repressor TetR was fused to the N-terminal half of PIF6, while PCM of PhyB was fused to the transactivation domain VP16. A reporter gene was placed under the control of a minimal human cytomegalovirus immediate early promoter fused to the upstream-located multiple repeats of the TetR-specific TetO operator (Figure 6d). This OT allowed gene expression to be spatiotemporally turned on with 660 nm and off with 740 nm light in a reversible manner. The system was compatible with different mammalian cell lines, including human primary cells, and was applied to spatially control angiogenesis in chicken embryos. However, addition of the exogenous PCB chromophore was required.

Table 3 presents a comparison between the OTs based on BphPs and plant phytochromes. In terms of future in vivo applications, the BphP-derived systems are advantageous over plant phytochromes because, similar to cryptochromes and the LOV and BLUF domains, they utilize the endogenous chromophore available in eukaryotic organisms. To overcome this limitation of plant phytochromes, engineering of mammalian cells to synthetize PCB has been suggested (91). Exhibiting the most redshifted absorbance over all chromophores (Figure 1), BV provides an additional advantage for deep-tissue penetration and lower scattering of the NIR light used to operate the BphP OTs.

Acknowledgments

This work was supported by grants GM073913, GM108579, and CA164468 from the US National Institutes of Health and ERC-2013-ADG-340233 from the European Union FP7 program.

Glossary

FP	fluorescent protein

Biosensor	or reporter; a molecule altering its fluorescence in response to changes in enzymatic activity metabolite concentration, or protein interaction
Optogenetic tool (OT)	a genetically encoded construct for light-mediated modulation of a desired cellular process
Photoreceptor	a protein–chromophore complex involved in light sensing and subsequent biochemical responses
Effector domain	domain in the photoreceptor that receives conformational changes of a photosensory core module and initiates biological responses, such as enzymatic activity or protein interaction
LOV domain	light-oxygen-voltage-sensing protein domain
BLUF domain	blue-light-utilizing FAD domain
FMN	flavin mononucleotide
FAD	flavin adenine dinucleotide
NIR	near-infrared
Phytochrome	photoreceptor found in plants and microbes that participates in their light-adaptive behavior, which incorporates bilin as a chromophore
Bilin	heme degradation derivative with linear arrangement of four pyrrole rings; also called linear tetrapyrrole
Photosensory core module (PCM)	a domain or several domains of photoreceptors, which bind chromophore and undergo primary conformational changes in response to light
Biliverdin IX α (BV)	a linear tetrapyrrole derivative of heme degradation catalyzed by heme oxygenase
Phycocyanobilin (PCB)	a linear tetrapyrrole derivative of biliverdin IXα reduction by ferredoxin oxidoreductase
BphP	bacterial phytochrome photoreceptor; also called bacterial phytochrome
PPI	protein–protein interaction
Reversibility	the ability of an optical tool to return to its inactive (ground, dark) state

LITERATURE CITED

1. van der Horst MA, Hellingwerf KJ. Photoreceptor proteins, “star actors of modern times”: a review of the functional dynamics in the structure of representative members of six different photoreceptor families. Acc Chem Res. 2004; 37:13–20. [PubMed: 14730990]

2. Christie JM, Gawthorne J, Young G, Fraser NJ, Roe AJ. LOV to BLUF: flavoprotein contributions to the optogenetic toolkit. Mol Plant. 2012; 5:533–44. [PubMed: 22431563]
3. Rockwell NC, Lagarias JC. A brief history of phytochromes. ChemPhysChem. 2010; 11:1172–80. [PubMed: 20155775]
4. Losi A, Gärtner W. The evolution of flavin-binding photoreceptors: an ancient chromophore serving trendy blue-light sensors. Annu Rev Plant Biol. 2012; 63:49–72. [PubMed: 22136567]
5. Chaves I, Pokorny R, Byrdin M, Hoang N, Ritz T, et al. The cryptochromes: blue light photoreceptors in plants and animals. Annu Rev Plant Biol. 2011; 62:335–64. [PubMed: 21526969]
6. Zhang F, Vierock J, Yizhar O, Fenno LE, Tsunoda S, et al. The microbial opsin family of optogenetic tools. Cell. 2011; 147:1446–57. [PubMed: 22196724]
7. Looger LL. Running in reverse: rhodopsins sense voltage. Nat Methods. 2012; 9:43–44. [PubMed: 22205516]
8. Gomelsky M, Klug G. BLUF: A novel FAD-binding domain involved in sensory transduction in microorganisms. Trends Biochem Sci. 2002; 27:497–500. [PubMed: 12368079]
9. Selby CP, Sancar A. The second chromophore in *Drosophila* photolyase/cryptochrome family photoreceptors. Biochemistry. 2012; 51:167–71. [PubMed: 22175817]
10. Ulijasz AT, Vierstra RD. Phytochrome structure and photochemistry: recent advances toward a complete molecular picture. Curr Opin Plant Biol. 2011; 14:498–506. [PubMed: 21733743]
11. Bellini D, Papiz MZ. Structure of bacteriophytochrome and light-stimulated protomer swapping with a gene repressor. Structure. 2012; 20:1436–46. [PubMed: 22795083]
12. Tarutina M, Ryjenkov DA, Gomelsky M. An unorthodox bacteriophytochrome from *Rhodobacter sphaeroides* involved in turnover of the second messenger c-di-GMP. J Biol Chem. 2006; 281:34751–58. [PubMed: 16968704]
13. Rockwell NC, Duanmu D, Martin SS, Bachy C, Price DC, et al. Eukaryotic algal phytochromes span the visible spectrum. PNAS. 2014; 111:3871–76. [PubMed: 24567382]
14. Giraud E, Verméglio A. Bacteriophytochromes in anoxygenic photosynthetic bacteria. Photosynth Res. 2008; 97:141–53. [PubMed: 18612842]
15. Auldridge ME, Forest KT. Bacterial phytochromes: more than meets the light. Crit Rev Biochem Mol Biol. 2011; 46:67–88. [PubMed: 21250783]
16. Piatkevich KD, Subach FV, Verkhusha VV. Engineering of bacterial phytochromes for near-infrared imaging, sensing, and light-control in mammals. Chem Soc Rev. 2013; 42:3441–52. Provides in-depth analysis and perspectives on the use of bacterial phytochromes for engineering of NIR optical tools including fluorescent proteins, biosensors, and optogenetic tools. [PubMed: 23361376]
17. Burgie ES, Bussell AN, Walker JM, Dubiel K, Vierstra RD. Crystal structure of the photosensing module from red/far-red light–absorbing plant phytochrome. PNAS. 2014; 111:10179–84. [PubMed: 24982198]
18. Takala H, Björling A, Berntsson O, Lehtivuori H, Niebling S, et al. Signal amplification and transduction in phytochrome photosensors. Nature. 2014; 509:245–48. [PubMed: 24776794]
19. Shcherbakova DM, Subach OM, Verkhusha VV. Red fluorescent proteins: advanced imaging applications and future design. Angew Chem Int Ed. 2012; 51:10724–38.
20. Salomon M, Christie JM, Knieb E, Lempert U, Briggs WR. Photochemical and mutational analysis of the FMN-binding domains of the plant blue light receptor, phototropin. Biochemistry. 2000; 39:9401–10. [PubMed: 10924135]
21. Drepper T, Eggert T, Circolone F, Heck A, Krauss U, et al. Reporter proteins for in vivo fluorescence without oxygen. Nat Biotechnol. 2007; 25:443–45. [PubMed: 17351616]
22. Walter J, Hausmann S, Drepper T, Puls M, Eggert T, Dihné M. Flavin mononucleotide-based fluorescent proteins function in mammalian cells without oxygen requirement. PLOS ONE. 2012; 7:e43921. [PubMed: 22984451]
23. Wingen M, Potzkei J, Endres S, Casini G, Rupprecht C, et al. The photophysics of LOV-based fluorescent proteins—new tools for cell biology. Photochem Photobiol Sci. 2014; 13:875–83. [PubMed: 24500379]

24. Chapman S, Faulkner C, Kaiserli E, Garcia-Mata C, Savenkov EI, et al. The photoreversible fluorescent protein iLOV outperforms GFP as a reporter of plant virus infection. PNAS. 2008; 105:20038–43. [PubMed: 19060199]
25. Christie JM, Hitomi K, Arvai AS, Hartfield KA, Mettlen M, et al. Structural tuning of the fluorscent protein iLOV for improved photostability. J Biol Chem. 2012; 287:22295–304. Describes advanced LOV-based fluorescent protein phiLOV 2.1 engineered using extensive structural and biochemical analyses. [PubMed: 22573334]
26. Shu X, Lev-Ram V, Deerinck TJ, Qi Y, Ramko EB, et al. A genetically encoded tag for correlated light and electron microscopy of intact cells, tissues, and organisms. PLOS Biol. 2011; 9:e1001041. Explores the photosensitizer properties of LOV-derived proteins to develop an FP serving as the singlet oxygen generator (miniSOG), which allowed correlative light and electron microscopy and chromophore-assisted light inactivation. [PubMed: 21483721]
27. Ruiz-González R, Cortajarena AL, Mejias SH, Agut M, Nonell S, Flors C. Singlet oxygen generation by the genetically encoded tag miniSOG. J Am Chem Soc. 2013; 135:9564–67. [PubMed: 23781844]
28. Lin JY, Sann SB, Zhou K, Nabavi S, Proulx CD, et al. Optogenetic inhibition of synaptic release with chromophore-assisted light inactivation (CALI). Neuron. 2013; 79:241–53. [PubMed: 23889931]
29. Qi YB, Garren EJ, Shu X, Tsien RY, Jin Y. Photo-inducible cell ablation in *Caenorhabditis elegans* using the genetically encoded singlet oxygen generating protein miniSOG. PNAS. 2012; 109:7499–504. [PubMed: 22532663]
30. Ryumina AP, Serebrovskaya EO, Shirmanova MV, Snopova LB, Kuznetsova MM, et al. Flavoprotein miniSOG as a genetically encoded photosensitizer for cancer cells. Biochim Biophys Acta. 2013; 1830:5059–67. [PubMed: 23876295]
31. Losi A, Gärtner W, Raffelberg S, Cella Zanacchi F, Bianchini P, et al. A photochromic bacterial photoreceptor with potential for super-resolution microscopy. Photochem Photobiol Sci. 2013; 12:231–35. [PubMed: 23047813]
32. Weissleder R. A clearer vision for in vivo imaging. Nat Biotechnol. 2001; 19:316–17. [PubMed: 11283581]
33. Auldridge ME, Satyshur KA, Anstrom DM, Forest KT. Structure-guided engineering enhances a phytochrome-based infrared fluorescent protein. J Biol Chem. 2012; 287:7000–9. [PubMed: 22210774]
34. Toh KC, Stojković EA, van Stokkum IH, Moffat K, Kennis JT. Fluorescence quantum yield and photochemistry of bacteriophytochrome constructs. Phys Chem Chem Phys. 2011; 13:11985–97. [PubMed: 21611667]
35. Sun YF, Xu JG, Tang K, Miao D, Gärtner W, et al. Orange fluorescent proteins constructed from cyanobacteriochromes chromophorylated with phycoerythrobilin. Photochem Photobiol Sci. 2014; 13:757–63. [PubMed: 24604419]
36. Yang X, Kuk J, Moffat K. Crystal structure of *Pseudomonas aeruginosa* bacteriophytochrome: photoconversion and signal transduction. PNAS. 2008; 105:14715–20. [PubMed: 18799746]
37. Fischer AJ, Lagarias JC. Harnessing phytochrome's glowing potential. PNAS. 2004; 101:17334–39. [PubMed: 15548612]
38. Fischer AJ, Rockwell NC, Jang AY, Ernst LA, Waggoner AS, et al. Multiple roles of a conserved GAF domain tyrosine residue in cyanobacterial and plant phytochromes. Biochemistry. 2005; 44:15203–15. [PubMed: 16285723]
39. Shu X, Royant A, Lin MZ, Aguilera TA, Lev-Ram V, et al. Mammalian expression of infrared fluorescent proteins engineered from a bacterial phytochrome. Science. 2009; 324:804–7. [PubMed: 19423828]
40. Yu D, Gustafson WC, Han C, Lafaye C, Noirclerc-Savoye M, et al. An improved monomeric infrared fluorescent protein for neuronal and tumour brain imaging. Nat Commun. 2014; 5:3626. [PubMed: 24832154]
41. Lehtivuori H, Rissanen I, Takala H, Bamford J, Tkachenko NV, Ihalainen JA. Fluorescence properties of the chromophore-binding domain of bacteriophytochrome from Deinococcus radiodurans. J Phys Chem B. 2013; 117:11049–57. [PubMed: 23464656]

42. Filonov GS, Piatkevich KD, Ting LM, Zhang J, Kim K, Verkhusha VV. Bright and stable near-infrared fluorescent protein for in vivo imaging. Nat Biotechnol. 2011; 29:757–61. [PubMed: 21765402]
43. Shcherbakova DM, Verkhusha VV. Near-infrared fluorescent proteins for multicolor in vivo imaging. Nat Methods. 2013; 10:751–54. Reports a series of spectrally distinct NIR FPs, called iRFPs, engineered from bacterial phytochromes, demonstrating their possibilities for noninvasive multicolor imaging in living animals. [PubMed: 23770755]
44. Jiguet-Jiglaire C, Cayol M, Mathieu S, Jeanneau C, Bouvier-Labit C, et al. Noninvasive near-infrared fluorescent protein-based imaging of tumor progression and metastases in deep organs and intraosseous tissues. J Biomed Opt. 2014; 19:16019. [PubMed: 24474505]
45. Sanders TA, Llagostera E, Barna M. Specialized filopodia direct long-range transport of SHH during vertebrate tissue patterning. Nature. 2013; 497:628–32. [PubMed: 23624372]
46. Zhu B, Wu G, Robinson H, Wilganowski N, Hall MA, et al. Tumor margin detection using quantitative NIRF molecular imaging targeting EpCAM validated by far red gene reporter iRFP. Mol Imaging Biol. 2013; 15:560–68. [PubMed: 23619897]
47. Krumholz A, Shcherbakova DM, Xia J, Wang LV, Verkhusha VV. Multicontrast photoacoustic in vivo imaging using near-infrared fluorescent proteins. Sci Rep. 2014; 4:3939. [PubMed: 24487319]
48. Zhang J, Wu XJ, Wang ZB, Chen Y, Wang X, et al. Fused-gene approach to photoswitchable and fluorescent biliproteins. Angew Chem Int Ed. 2010; 49:5456–58.
49. Piatkevich KD, Subach FV, Verkhusha VV. Far-red light photoactivatable near-infrared fluorescent proteins engineered from a bacterial phytochrome. Nat Commun. 2013; 4:2153. [PubMed: 23842578]
50. Potzkei J, Kunze M, Drepper T, Gensch T, Jaeger KE, Büchs J. Real-time determination of intracellular oxygen in bacteria using a genetically encoded FRET-based biosensor. BMC Biol. 2012; 10:28. [PubMed: 22439625]
51. Gu Z, Zhao M, Sheng Y, Bentolila LA, Tang Y. Detection of mercury ion by infrared fluorescent protein and its hydrogel-based paper assay. Anal Chem. 2011; 83:2324–29. [PubMed: 21323346]
52. Filonov GS, Verkhusha VV. A near-infrared BiFC reporter for in vivo imaging of protein-protein interactions. Chem Biol. 2013; 20:1078–86. Describes the first NIR reporter for studies of PPIs by bimolecular fluorescence complementation assay, called iSplit, which enabled noninvasive imaging of model interactions in living animals. [PubMed: 23891149]
53. Tchekanda E, Sivanesan D, Michnick SW. An infrared reporter to detect spatiotemporal dynamics of protein-protein interactions. Nat Methods. 2014; 11:641–44. [PubMed: 24747815]
54. Stepanenko OV, Bublikov GS, Stepanenko OV, Shcherbakova DM, Verkhusha VV, et al. A knot in the protein structure—probing the near-infrared fluorescent protein iRFP designed from a bacterial phytochrome. FEBS J. 2014; 281:2284–98. [PubMed: 24628916]
55. Strickland D, Yao X, Gawlak G, Rosen MK, Gardner KH, Sosnick TR. Rationally improving LOV domain–based photoswitches. Nat Methods. 2010; 7:623–26. [PubMed: 20562867]
56. Strickland D, Moffat K, Sosnick TR. Light-activated DNA binding in a designed allosteric protein. PNAS. 2008; 105:10709–14. [PubMed: 18667691]
57. Zoltowski BD, Vaccaro B, Crane BR. Mechanism-based tuning of a LOV domain photoreceptor. Nat Chem Biol. 2009; 5:827–34. [PubMed: 19718042]
58. Wu YI, Wang X, He L, Montell D, Hahn KM. Spatiotemporal control of small GTPases with light using the LOV domain. Methods Enzymol. 2011; 497:393–407. [PubMed: 21601095]
59. Hahn KM, Kuhlman B. Hold me tightly LOV. Nat Methods. 2010; 7:595–597. [PubMed: 20676078]
60. Zoltowski BD, Schwerdtfeger C, Widom J, Loros JJ, Bilwes AM, et al. Conformational switching in the fungal light sensor Vivid. Science. 2007; 316:1054–57. [PubMed: 17510367]
61. Zoltowski BD, Crane BR. Light activation of the LOV protein vivid generates a rapidly exchanging dimer. Biochemistry. 2008; 47:7012–19. [PubMed: 18553928]
62. Sawa M, Nusinow DA, Kay SA, Imaizumi T. FKF1 and GIGANTEA complex formation is required for day-length measurement in *Arabidopsis*. Science. 2007; 318:261–65. [PubMed: 17872410]

63. Wu YI, Frey D, Lungu OI, Jaehrig A, Schlichting I, et al. A genetically encoded photoactivatable Rac controls the motility of living cells. Nature. 2009; 461:104–8. [PubMed: 19693014]
64. Mills E, Chen X, Pham E, Wong S, Truong K. Engineering a photoactivated caspase-7 for rapid induction of apoptosis. ACS Synth Biol. 2012; 1:75–82. [PubMed: 23651071]
65. Lungu OI, Hallett RA, Choi EJ, Aiken MJ, Hahn KM, Kuhlman B. Designing photoswitchable peptides using the *As*LOV2 domain. Chem Biol. 2012; 19:507–17. [PubMed: 22520757]
66. Strickland D, Lin Y, Wagner E, Hope CM, Zayner J, et al. TULIPs: tunable, light-controlled interacting protein tags for cell biology. Nat Methods. 2012; 9:379–84. Describes the LOV domain–based TULIP system, which allows the control of versatile protein interactions with spatiotemporal resolution. [PubMed: 22388287]
67. Wang X, Chen X, Yang Y. Spatiotemporal control of gene expression by a light-switchable transgene system. Nat Methods. 2012; 9:266–69. [PubMed: 22327833]
68. Motta-Mena LB, Reade A, Mallory MJ, Glantz S, Weiner OD, et al. An optogenetic gene expression system with rapid activation and deactivation kinetics. Nat Chem Biol. 2014; 10:196–202. [PubMed: 24413462]
69. Zoltowski BD, Motta-Mena LB, Gardner KH. Blue light-induced dimerization of a bacterial LOV-HTH DNA-binding protein. Biochemistry. 2013; 52:6653–61. [PubMed: 23992349]
70. Grusch M, Schelch K, Riedler R, Reichhart E, Differ C, et al. Spatio-temporally precise activation of engineered receptor tyrosine kinases by light. EMBO J. 2014; 33:1713–26. [PubMed: 24986882]
71. Yazawa M, Sadaghiani AM, Hsueh B, Dolmetsch RE. Induction of protein-protein interactions in live cells using light. Nat Biotechnol. 2009; 27:941–45. [PubMed: 19801976]
72. Polstein LR, Gersbach CA. Light-inducible gene regulation with engineered zinc finger proteins. Methods Mol Biol. 2014; 1148:89–107. [PubMed: 24718797]
73. Schröder-Lang S, Schwärzel M, Seifert R, Strünker T, Kateriya S, et al. Fast manipulation of cellular cAMP level by light in vivo. Nat Methods. 2007; 4:39–42. [PubMed: 17128267]
74. Stierl M, Stumpf P, Udwari D, Gueta R, Hagedorn R, et al. Light modulation of cellular cAMP by a small bacterial photoactivated adenylyl cyclase, bPAC, of the soil bacterium *Beggiatoa*. J Biol Chem. 2011; 286:1181–88. [PubMed: 21030594]
75. Ryu MH, Moskvin OV, Siltberg-Liberles J, Gomelsky M. Natural and engineered photoactivated nucleotidyl cyclases for optogenetic applications. J Biol Chem. 2010; 285:41501–8. [PubMed: 21030591]
76. Bugaj LJ, Choksi AT, Mesuda CK, Kane RS, Schaffer DV. Optogenetic protein clustering and signaling activation in mammalian cells. Nat Methods. 2013; 10:249–52. [PubMed: 23377377]
77. Wend S, Wagner HJ, Müller K, Zurbriggen MD, Weber W, Radziwill G. Optogenetic control of protein kinase activity in mammalian cells. ACS Synth Biol. 2014; 3:280–85. [PubMed: 24090449]
78. Kim N, Kim JM, Lee M, Kim CY, Chang KY, Heo WD. Spatiotemporal control of fibroblast growth factor receptor signals by blue light. Chem Biol. 2014; 21:903–12. [PubMed: 24981772]
79. Idevall-Hagren O, Dickson EJ, Hille B, Toomre DK, De Camilli P. Optogenetic control of phosphoinositide metabolism. PNAS. 2012; 109:e2316–23. [PubMed: 22847441]
80. Lee S, Park H, Kyung T, Kim NY, Kim S, et al. Reversible protein inactivation by optoge-netic trapping in cells. Nat Methods. 2014; 11:633–36. Homo-oligomerization of CRY2, followed by its heterodimerization with its CIB1 partner, was efficiently applied for inhibition of protein activity by its light-inducible trapping in clusters. [PubMed: 24793453]
81. Konermann S, Brigham MD, Trevino AE, Hsu PD, Heidenreich M, et al. Optical control of mammalian endogenous transcription and epigenetic states. Nature. 2013; 500:472–76. Applies the LITE system, consisting of CRY2 with TALE fusion, for modulation of mammalian endogenous gene expression and targeted epigenetic chromatin modifications. [PubMed: 23877069]
82. Ryu MH, Kang IH, Nelson MD, Jensen TM, Lyuksyutova AI, et al. Engineering adenylate cyclases regulated by near-infrared window light. PNAS. 2014; 111:10167–72. [PubMed: 24982160]

83. Weissenberger S, Schultheis C, Liewald JF, Erbguth K, Nagel G, Gottschalk A. PAC*a*–an optogenetic tool for in vivo manipulation of cellular cAMP levels, neurotransmitter release, and behavior in *Caenorhabditis elegans*. J Neurochem. 2011; 116:616–25. [PubMed: 21166803]
84. Gasser C, Taiber S, Yeh CM, Wittig CH, Hegemann P, et al. Engineering of a red-light-activated human cAMP/cGMP-specific phosphodiesterase. PNAS. 2014; 111:8803–8. Describes the bacteriophytochrome-based NIR-light-activated phosphodiesterase, which enabled degradation of second messengers such as cGMP and cAMP in a light-controllable manner. [PubMed: 24889611]
85. Pandit J, Forman MD, Fennell KF, Dillman KS, Menniti FS. Mechanism for the allosteric regulation of phosphodiesterase 2A deduced from the X-ray structure of a near full-length construct. PNAS. 2009; 106:18225–30. [PubMed: 19828435]
86. Ni M, Tepperman JM, Quail PH. Binding of phytochrome B to its nuclear signalling partner PIF3 is reversibly induced by light. Nature. 1999; 400:781–84. [PubMed: 10466729]
87. Zhu Y, Tepperman JM, Fairchild CD, Quail PH. Phytochrome B binds with greater apparent affinity than phytochrome A to the basic helix-loop-helix factor PIF3 in a reaction requiring the PAS domain of PIF3. PNAS. 2000; 97:13419–24. [PubMed: 11069292]
88. Shimizu-Sato S, Huq E, Tepperman JM, Quail PH. A light-switchable gene promoter system. Nat Biotechnol. 2002; 20:1041–44. [PubMed: 12219076]
89. Levskaya A, Weiner OD, Lim WA, Voigt CA. Spatiotemporal control of cell signalling using a light-switchable protein interaction. Nature. 2009; 461:997–1001. [PubMed: 19749742]
90. Müller K, Engesser R, Metzger S, Schulz S, Kämpf MM, et al. A red/far-red light–responsive bi-stable toggle switch to control gene expression in mammalian cells. Nucleic Acids Res. 2013; 41:e77. Describes the first NIR-light optogenetic tool based on reversible PhyB–PIF6 interactions for control of gene expression in mammalian cells, which requires a supply of exogenous PCB chromophore. [PubMed: 23355611]
91. Müller K, Engesser R, Timmer J, Nagy F, Zurbriggen MD, Weber W. Synthesis of phycocyanobilin in mammalian cells. Chem Commun. 2013; 49:8970–72.
92. Guo Q, Wang X, Tibbitt MW, Anseth KS, Montell DJ, Elisseeff JH. Light activated cell migration in synthetic extracellular matrices. Biomaterials. 2012; 33:8040–46. [PubMed: 22889487]
93. Peter E, Dick B, Baeurle SA. Signaling pathway of a photoactivable Rac1-GTPase in the early stages. Proteins. 2012; 80:1350–62. [PubMed: 22275005]
94. Rao MV, Chu PH, Hahn KM, Zaidel-Bar R. An optogenetic tool for the activation of endogenous diaphanous-related formins induces thickening of stress fibers without an increase in contractility. Cytoskeleton. 2013; 70:394–407. [PubMed: 23677607]
95. Kennedy MJ, Hughes RM, Peteya LA, Schwartz JW, Ehlers MD, Tucker CL. Rapid blue-light-mediated induction of protein interactions in living cells. Nat Methods. 2010; 7:973–75. [PubMed: 21037589]

SUMMARY POINTS

1. The main advantages of FPs designed from LOV domains over GFP-like probes are their smaller size and functionality in anaerobic conditions. In the presence of oxygen, LOV-based FPs generate ROS and can be applied for correlative light and electron microscopy or for photoinactivation of proteins and whole cells.
2. NIR FPs and PPI reporters engineered from BphPs enable noninvasive whole-body imaging in mammals. BphP-based FPs differ in their efficiency and specificity for the BV chromophore. Whereas iRFPs rely solely on exogenous BV present in mammalian tissues, FPs with poor BV incorporation require its exogenous supply or coexpression of heme oxygenase for its additional intracellular synthesis.
3. OTs engineered from LOV domains and CRY2 possess convenient features for versatile applications in blue-light-driven PPIs, endogenous gene transcription activation, and regulation of enzyme activities. Owing to the small size of the photosensory units, both the light sensitivity and the dynamic range of resultant OTs may be tuned. The use of potentially phototoxic blue light with restricted tissue penetration limits their use in in vivo applications.
4. The most redshifted OTs are based on phytochromes. Photocontrollable interaction of plant phytochromes with their interacting partners was applied to spatiotemporally control cell signaling and gene expression. However, the intracellular unavailability of PCB chromophore presents a drawback of OTs derived from plant phytochromes. OTs based on bacterial phytochromes are promising alternatives for in vivo applications, thanks to their use of the endogenous BV chromophore and NIR-light absorbance.

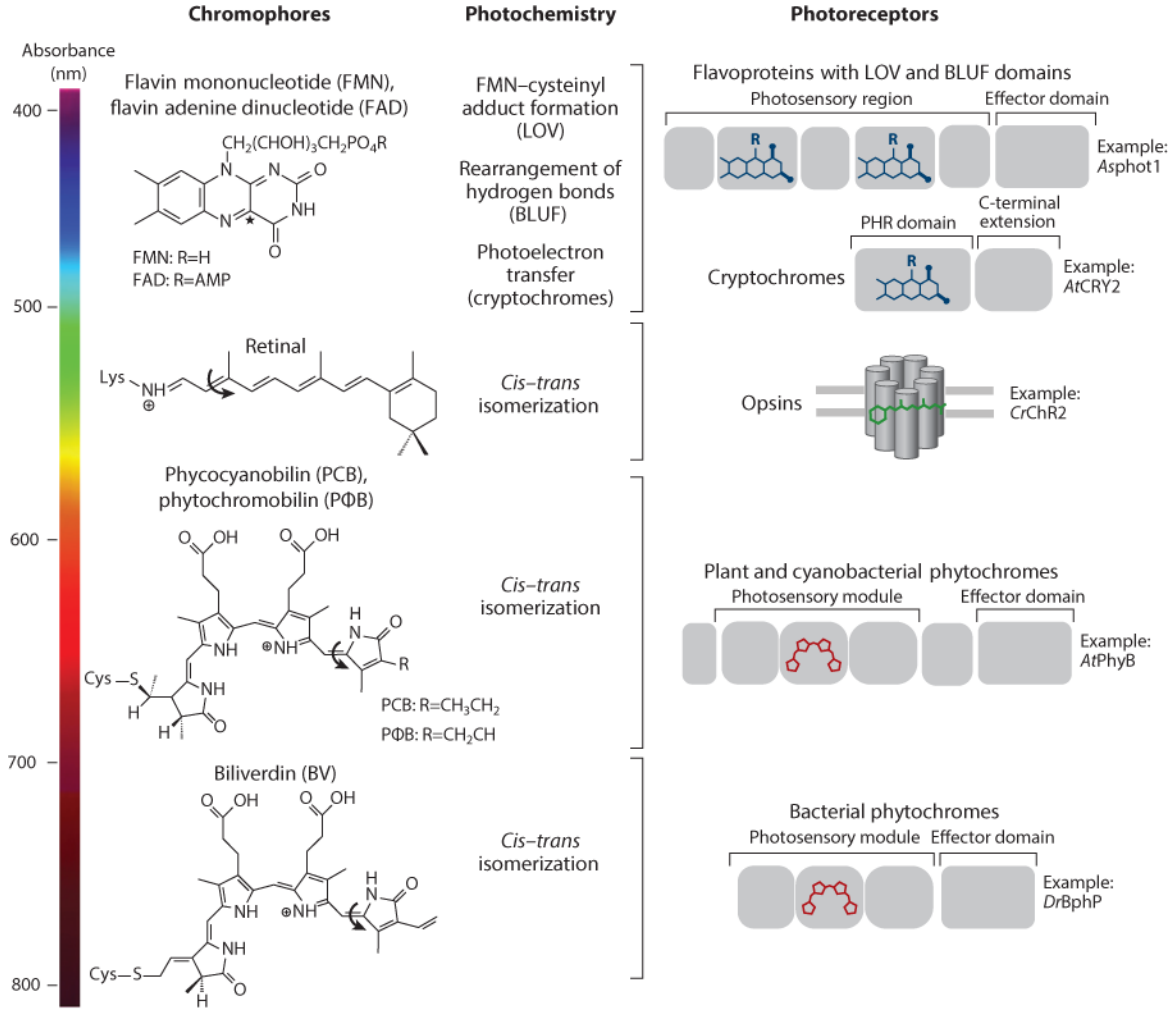

Figure 1.

A variety of photoreceptors and their chromophores explored as templates to engineer optical tools. (*Left*) Chemical structures of the chromophores and a color-scale bar representing the wavelength range of their absorbance in natural photoreceptors. The chromophores are presented in their inactive (dark) states. The retinal structure corresponds to microbial opsins. For each chromophore, its primary photochemistry is indicated. An asterisk indicates the C4a atom in FMN, which forms a covalent bond with a conservative cysteine in LOV domains upon light illumination. The arrow in some chemical structures indicates the double bond that isomerizes upon activation. (*Right*) Natural photoreceptors that have been actively explored to develop genetically encoded optical tools. For each type of photoreceptor, a schematic domain structure of one example receptor is presented. Note that all photoreceptors, except opsins, have a modular domain organization with separate photosensory module and effector domain. Abbreviations: AMP, adenosine 5′-monophosphate; *As*phot1, *Avena sativa* phototropin 1; *At*CRY2, *Arabidopsis thaliana* cryptochrome 2; *At*PhyB, *A. thaliana* phytochrome B; BLUF, blue-light-utilizing flavin adenine dinucleotide; *Cr*ChR2, *Chlamydomonas reinhardtii* channelrhodopsin-2; *Dr*BphP, *Deinococcus radiodurans* bacterial phytochrome; LOV, light-oxygen-voltage-sensing.

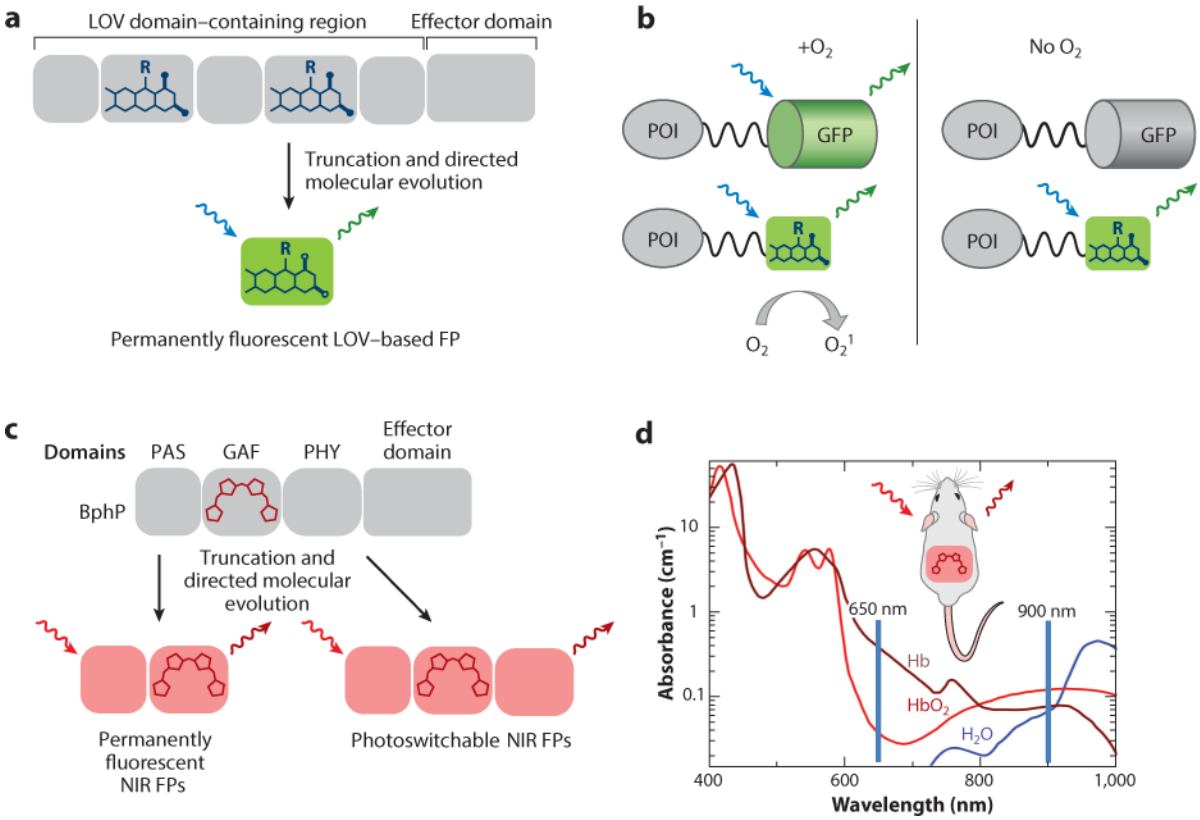

Figure 2.

Engineering of FPs from photoreceptors and their advantages over GFP-like FPs. (*a*) Strategy for engineering of LOV domain–based FPs. The truncated LOV domain is subjected to molecular evolution to block FMN–cysteinyl adduct formation and improve brightness and chromophore incorporation. (*b*) LOV domain–based FPs are small (~10–15 kDa) and do not require molecular oxygen for maturation. Thus, they can be utilized in applications as small fusion tags and as reporters in anaerobic conditions. In the presence of oxygen, LOV domain–based FPs generate reactive oxygen species (singlet oxygen) and, thus, can serve as photosensitizers for photodestruction of proteins and cells. (*c*) Strategy for engineering of permanently fluorescent and photoswitchable NIR FPs. To abolish photoswitching and obtain a permanently fluorescent FP, the phytochrome is truncated to chromophore-binding PAS and GAF domains. Directed molecular evolution allows one to improve the brightness, efficiency, and specificity of BV incorporation. For development of photoactivatable FPs, the PHY domain is not deleted to preserve photoswitchable properties. In molecular evolution, variants that do not photoswitch from fluorescent Pr form under weak illumination during imaging are selected. (*d*) The main advantage of FPs derived from bacterial phytochromes is their NIR-shifted spectra. In the NIR transparency window (650–900 nm), mammalian tissues are most transparent to light because combined absorption of hemoglobin and water is minimal. Thus, NIR FPs are suitable for noninvasive whole-body imaging. Abbreviations: FMN, flavin mononucleotide; FP, fluorescent protein; GAF, cGMP phosphodiesterase/adenylate cyclase/FhlA; GFP, green fluorescent protein; LOV, light-

oxygen-voltage-sensing; NIR, near-infrared; PAS, Per–Arnt–Sim; PHY, phytochrome-specific; POI, protein of interest.

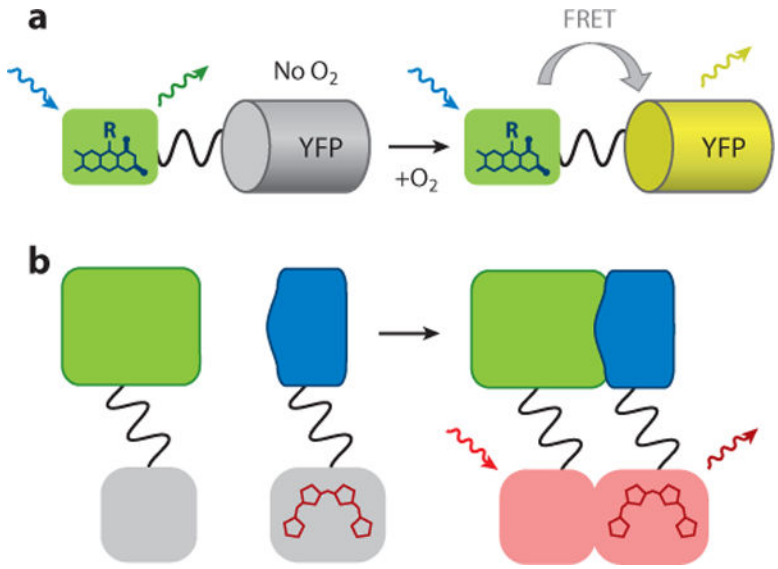

Figure 3.

Fluorescent reporters designed from photoreceptors. (*a*) A LOV-based reporter for oxygen. In anaerobic conditions, YFP does not form a chromophore, and no FRET between LOV-based FP and YFP occurs. In the presence of oxygen, a YFP chromophore is formed, and the matured YFP acts as a FRET acceptor for the LOV-based FP. The process is not reversible. Thus, intracellular stability and turnover of reporter influence its response and its kinetics. (*b*) Phytochrome-based reporters for protein–protein interactions using a bimolecular fluorescence complementation approach. Upon interaction of two protein partners, the fused PAS and GAF phytochrome domains complement into a functional FP. Abbreviations: FP, fluorescent protein; FRET, Förster resonance energy transfer; GAF, cGMP phosphodiesterase/adenylate cyclase/FhlA; LOV, light-oxygen-voltage-sensing; PAS, Per–Arnt–Sim; YFP, yellow fluorescent protein.

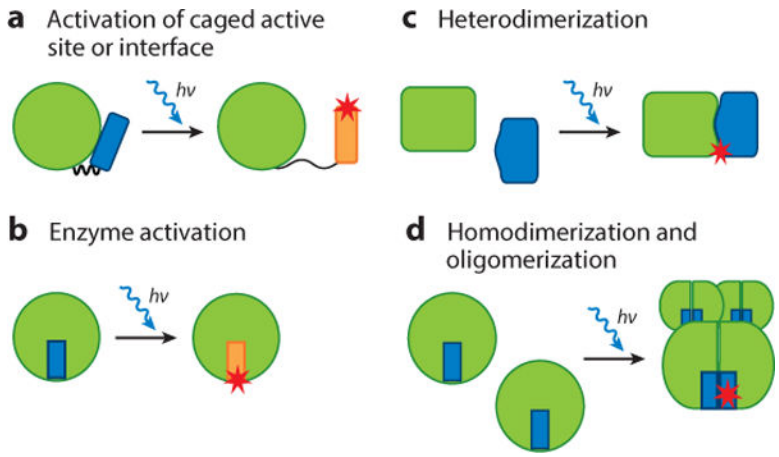

Figure 4.

General strategies to engineer optogenetic tools. (*a*) Caging the protein interaction interface/enzyme active site inhibits protein activity in darkness. During light absorption, photoreceptors or light-sensitive domains can undergo structural rearrangements and uncage the interface/active site of the caged protein in the lit state. (*b*) Light-induced structural changes in the photosensory core may lead to tertiary structure perturbations in the whole protein molecule and activate effector domain. (*c*,*d*) After light illumination, the quaternary structure of photoreceptors can change. They can (*c*) hetero-oligomerize or (*d*) homo-oligomerize and may control interaction of fused protein partners, reconstitute split enzymes, or relocalize fused proteins to other cell compartments. The term *hv* designates the activation light. The red asterisk indicates an activated state.

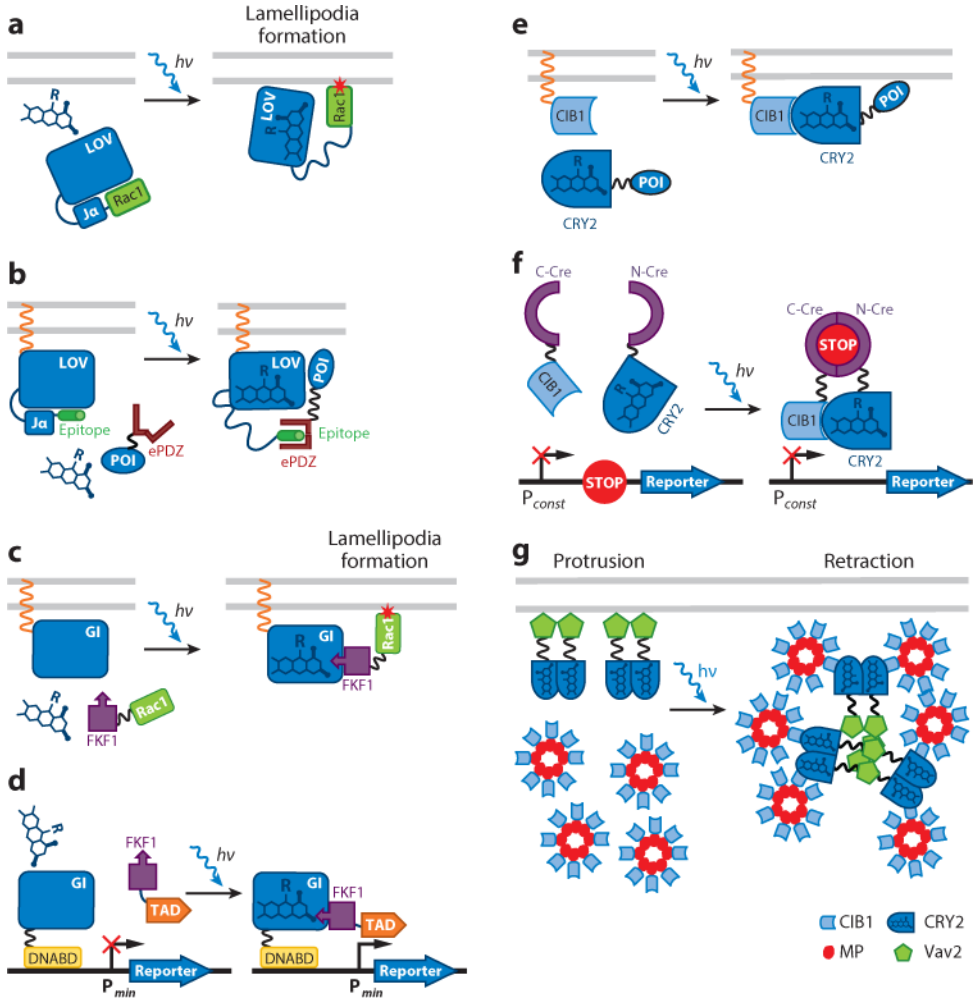

Figure 5.

Optogenetic constructs that are activated by blue light. (*a*) After illumination of asLOV2–Rac1 [*Avena sativa* LOV (light-oxygen-voltage-sensing) domain 2] fusion, FMN (flavin mononucleotide) binding occurs, and Rac1, which was caged on the asLOV2 core, is released. This process induces lamellipodia formation through actin polymerization. (*b*) TULIP (tunable light-induced dimerization tags) technology is based on interaction of the ePDZ (enhanced postsynaptic density protein 95, disc-large tumor suppressor protein, zonula occludens 1) domain with its binding epitope caged on the asLOV2 core in the dark state. Illumination induces structural changes in asLOV2, and unwinding of the Jα helix results in the availability of a binding epitope for ePDZ. Thus, a protein fused to the ePDZ domain can be translocated to a specific cell compartment and perform its function. (*c*) Light-induced interaction between GIGANTEA (GI) and FKF1 (flavin-binding kelch repeat F-box 1) proteins and their heterodimerization result in lamellipodia formation through attraction of Rac1 fused with FKF1 to the plasma membrane. (*d*) For light-induced transcription activation, GI is fused to the DNA-binding domain (Gal4) and FKF1 is fused to the transcription activation domain (TAD). In the lit state, GI interacts with FKF1, and transcription activation by TAD occurs from the minimal promoter (P_{min}). (*e*) A protein of interest (POI) can be recruited to the plasma membrane by fusing it to cryptochrome 2

(CRY2), which interacts with its membrane-anchored partner CIB1 [CRY-interacting bHLH1 (helix-loop-helix 1)] upon illumination. (*f*) After illumination, reconstitution of split Cre recombinase occurs when the N-terminal part of Cre is fused to CRY2 and the C-terminal part of Cre is fused to CIB1. Reconstituted Cre removes the terminator region (STOP) flanked by loxP sites and activates reporter gene transcription from the constitutive promoter (P_{const}). (*g*) Cell morphology can be controlled by light-induced clustering of Vav2, a guanine nucleotide exchange factor that activates Rho small GTPases. In the dark state, the Vav2–CRY2 fusion is localized near the plasma membrane and induces protrusion formation. In the lit state, CRY2 interacts with CIB1 fused with the multimeric protein (MP), and formation of large clusters occurs, thus inhibiting Vav2 in clusters and causing retraction of the plasma membrane. The term *hv* designates the activation light.

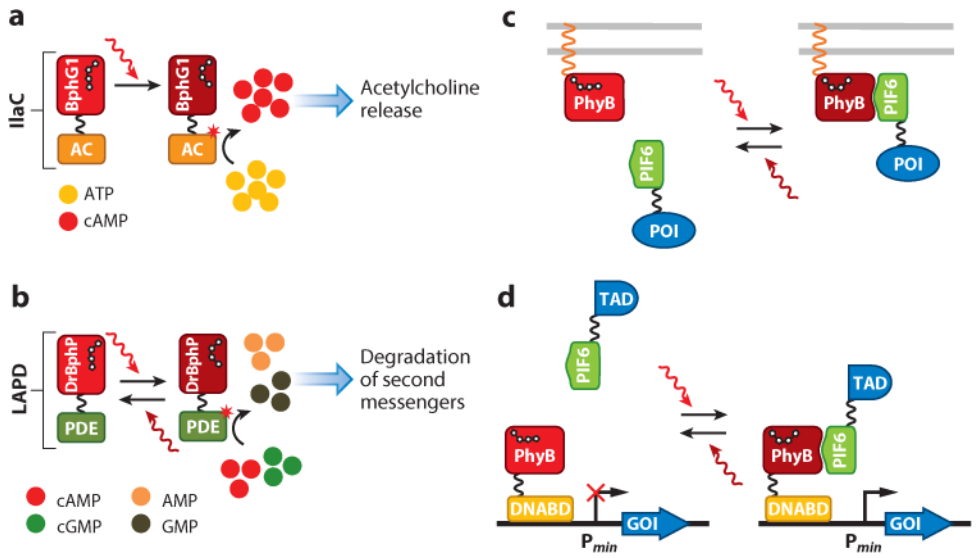

Figure 6.

Optogenetic tools based on phytochromes. (*a*) Near-infrared (NIR) light–activated adenylate cyclase (IlaC) consists of a photosensory module of *Rhodobacter sphaeroides* BphP (bacterial phytochrome), BphG1, and the AC (adenylate cyclase) domain from *Nostoc* sp. CyaB1. Synthesis of cAMP by IlaC can be activated with NIR light. When expressed in cholinergic neurons of *Caenorhabditis elegans*, it affects worm behavior in a light-dependent manner by increasing intracellular cAMP, which leads to release of acetylcholine and subsequent activation of muscles. (*b*) Light-activated phosphodiesterase (LAPD) is designed by fusing the photosensory module of *Deinococcus radiodurans* BphP with the effector domain of human phosphodiesterase 2A (PDE). Upon NIR illumination, phosphodiesterase becomes active and upregulates hydrolysis of second messengers, such as cAMP and cGMP. (*c*) Light-controllable reversible interaction of PhyB and phytochrome-interacting factor 6 (PIF6) can be exploited for recruitment of the protein of interest (POI) to the plasma membrane. After 650-nm light illumination, PhyB undergoes structural rearrangements and interacts with PIF6. This interaction is reversible, and dissociation can be activated by 750-nm light. (*d*) Light-induced heterodimerization can be used for transcription activation of the gene of interest (GOI) from the minimal promoter (P_{min}). PhyB is fused to the DNA-binding domain (DNABD), and PIF6 is fused to the transcription activation domain (TAD). Upon 660-nm light illumination, PhyB and PIF6 interact, and TAD activates transcription from the P_{min}. Dissociation of the PhyB–PIF6 pair can be activated by 740-nm light, and the system can be reversibly toggled between the stable on (transcription is activated) and off (transcription is terminated) states. The asterisk indicates an activated state.

Annu Rev Biochem. Author manuscript; available in PMC 2015 December 16.

Table 1

Fluorescent proteins (FPs) engineered from photoreceptors for applications in mammalian cells

LOV-based FPs

FP	Natural photoreceptor used as template	Excitation (nm); emission (nm)	Extinction coefficient (M^{-1} cm^{-1})	Quantum yield (%)	Molecular weight; oligomeric state	Demonstrated applications	Specific properties related to applications	Reference
iLOV	*At*phot2	447, ~470; 497, (~530)	12,500[a]	44	~10 kDa; monomeric	Fluorescent imaging of fused proteins in applications, in which steric constraints may affect protein function	Low photostability; photobleaching is reversible	24
phiLOV2.1	*At*phot2	447, ~470; 496, (524)	ND	ND		Similar to that for iLOV	Greater photostability than in iLOV	25
miniSOG	*At*phot2	448, 473; 500, (528)	16,700 at 448 nm; 13,600 at 473 nm	37	15 kDa; monomeric	Correlative electron microscopy and fluorescence imaging; photoinactivation of proteins and photodestruction of cells	Specifically optimized to generate singlet oxygen species	26
*Pp*FbFP	*Pp*SB2	450, ~470; 495, (~525)	12,500[a]	17	19 kDa; dimeric	Genetically encoded reporters for use in anaerobic conditions	The protein is dimeric and relatively dim	21
*Ec*FbFP	*Bs*YtvA	450, ~470; 495, (~525)	12,500[a]	39			The protein is dimeric	21

BphP-based FPs

FP	Natural photoreceptor used as template	Excitation (nm)[c]; emission (nm)	Extinction coefficient (M^{-1} cm^{-1})	Quantum yield (%)	Molecular weight; oligomeric state	Cellular brightness, relative to iRFP713 (%)[e]	Demonstrated applications	Specific properties related to applications	Reference(s)
IFP1.4	*Dr*BphP	684; 708	92,000 (102,000)[d]	7.7 (7.0)[d]	35 kDa; monomeric	8 (increased to 14 after 2-h incubation with 25 μM BV)	Whole-body imaging of liver	Supply of exogenous BV chromophore is required	39
IFP2.0	*Dr*BphP	690; 711	86,125	8.0	35 kDa; dimeric[g]	<8 g (without supply of exogenous BV) ~100 (with coexpressed heme oxygenase)	Whole-body imaging of tumors, imaging of tissues in *Drosophila*· larva	Requires coexpression of heme oxygenase or supply of exogenous BV chromophore	40

BphP-based FPs									
FP	**Natural photoreceptor used as template**	**Excitation (nm)[c]; emission (nm)**	**Extinction coefficient (M^{-1} cm^{-1})**	**Quantum yield (%)**	**Molecular weight; oligomeric state**	**Cellular brightness, relative to iRFP713 (%)[e]**	**Demonstrated applications**	**Specific properties related to applications**	**Reference(s)**
iRFP670	*Rp*BphP6	643; 670	114,000	11.1	35 kDa; dimeric	119	Whole-body multicolor fluorescence imaging, multicontrast photoacoustic tomography in vivo	Efficient binding of endogenous BV chromophore in many mammalian cell types and tissues. No need for supply of exogenous BV or coexpression of heme oxygenase	42, 43
iRFP682	*Rp*BphP2	663; 682	90,000	11.3		105			
iRFP702	*Rp*BphP6	673; 702	93,000	8.2		61			
iRFP713	*Rp*BphP2	690; 713	98,000	6.3		100			
iRFP720	*Rp*BphP2	702; 720	96,000	6.0		110			
PAiRFPl	*At*BphP2	690[h]; 717[h]	67,100	4.8	57 kDa; dimeric	25 (increased to 43 after 2 h with 25 μM BV)	Whole-body imaging with enhanced signal-to-background ratio in auto-fluorescent tissues	Photoactivatable by both far-red and MR light. Half-time of thermal relaxation to dark state is ~1 h	49
PAiRFP2	*At*BphP2	692[h]; 719[h]	63,600	4.7		7 (increased to 9 after 2 h with 25 μM BV)		Photoactivatable by both far-red and MR light. Half-time of thermal relaxation to dark state is ~4 h	

[a] Extinction coefficient corresponds to the molar extinction coefficient of free flavin mononucleotide (FMN) at 450 nm.

[b] Shoulder or minor peaks are shown in parentheses.

[c] A11 phytochrome-related FPs can also be excited at the Soret band (~400 nm), corresponding to the absorbance of a pyrrole ring.

[d] Measured in Reference 42.

[e] Determined as effective fluorescence in HeLa cells relative to iRFP713 with no supply of exogenous biliverdin (BV). The values may vary in different cell types owing to variations in endogenous BV concentration and protein expression level.

[f] Monomeric state was shown by size-exclusion chromatography; localization of fusions proteins in cells has not been demonstrated.

[g] Our size-exclusion chromatography and mammalian cell expression data.

[h] Corresponds to a photoactivated state.

Abbreviations: Asphot2, *Avena sativa* phototropin 2; AtBphP2, *Agrobacterium tumefaciens* bacterial phytochrome 2; *Bs*YtvA, *Bacillus subtilis* YtvA; *Dr*BphP, *Deinococcus radiodurans* bacterial phytochrome; LOV, light-, oxygen-, voltage-sensing; ND, not determined; NIR, near-infrared; *Pp*SB2, *Pseudomonas putida* SB2; *Rp*BphP2 and *Rp*BphP6, *Rhodopseudomonas palustris* bacterial phytochrome 2 and 6, respectively.

Table 2

Fluorescent biosensors and reporters engineered from photoreceptors for applications in mammalian cells

Reporter for oxygen

Reporter	FPs used in design (excitation, nm; emission, nm)	Readout	Dynamic range	Sensed concentrations	Advantages	Limitations	Reference
FluBO	EcFbFP (450, 495); YFP (512, 528)	Ratiometric FRET, donor lifetime FRET	Apparent FRET efficiency is 37%	0–0.08 mmol/L	Noninvasive intracellular detection	Oxygen-dependent chromophore formation in YFP is irreversible	50

Biosensor for mercury

Reporter	FPs used in design (excitation, nm; emission, nm)	Readout	Dynamic range	Sensed concentrations	Advantages	Limitations	Reference
IFP1.4	IFP1.4 (684, 708)	Fluorescence of IFP1.4 affected by Hg^{2+}	0–100%	>20 μM (in mammalian cells)	First genetically encoded Hg^{2+} sensor	Low sensitivity in mammalian cells	51

Reporters for PPI (protein complementation assay)

Reporter	FPs used in design (excitation, nm; emission, nm)	Extinction coefficient (M^{-1} cm^{-1})	Quantum yield (%)	Contrast in cultured mammalian cells, fold	Interacting pairs tested	Advantages	Limitations	Reference
iSplit	iRFP713 (690, 713)	85,500	6.8	>20–50 (~18 in mice)	E-coil with K-coil, FRB with FKBP	High brightness and large complementation contrast. Applicable for in vivo PPI studies	Irreversible	52
IFP PCA	IFP1.4 (684, 708)	42,890	6.2	Up to 2 (>20–50 in yeast)	Protein kinase A subunits, SHC1 with GRB2, some known PPIs in yeast	Apparent reversibility. Suitable for imaging of spatiotemporal dynamics of PPIs	Low brightness and complementation contrast in mammalian cells. Requires supply of exogenous BV	53

Abbreviations: BV, biliverdin; FP, fluorescent protein; FKBP, FK506-binding protein; FRB, FKBP-rapamycin binding; FRET, Förster resonance energy transfer; GRB2, growth factor receptor–bound protein 2; PPI, protein–protein interaction; SHC1, Src homology 2 domain–containing transforming protein 1; YFP, yellow fluorescent protein.

Table 3

Major characteristics of optogenetic systems with applicability in eukaryotic cells

Optogenetic tool	Photoreceptor or domain	Chromophore	Mechanism of action	Expression system	Activation light	Type of application	Limitations	Reference(s)
LOV domains								
LOV2-Racl (PA-Racl)	*As*LOV2	FMN	Release of steric inhibition of GTPase	Mammalian cells	Blue	Protein activation, cell migration	Applicable only to Rac1-dependent regulation pathways	63, 92, 93
LOV2-ipaA, LOV2-SsrA			Uncaging of interacting epitope	Yeast cells		Transcription activation (*As*LOV2–ipaA)	Not applied to mammalian cells	65
L57V			Uncaging of effector epitope	Mammalian cells		Induction of apoptosis	Applicable only to apoptosis-mediated cell death	64
LAD	FKF1					Interaction between GI and LOV domain of FKF1	Protein interaction, gene expression	Large size of involved proteins 71
TULIP	*As*LOV2		Uncaging of interacting epitope	Mammalian cells, yeast cells		Protein interaction, MAPK cascade activation	System was applied only for translocation-mediated regulation of protein interaction	66
LITEZ	FKF1		Interaction between GI and LOV domain of FKF1	Mammalian cells		Transcription activation	Decreased response with reduction of ZFP-binding motif repeat number	72
LightON	WD	FAD	Homodimerization	Mammalian cells, transgenic mice		Transcription activation	Applicable only to proteins that require dimerization for activation	67
PA-DAD	*As*LOV2	FMN	Release of steric inhibition of DAD	Mammalian cells		Transcription activation, cell morphology regulation	Low dynamic range	94
EL222	*El*LOV		Homodimerization	Mammalian cells, zebrafish embryos		Transcription activation	Reporter gene activates only under $(C20)_x$-repeat element control	68
Opto-RTK	*Vf*LOV			Mammalian cells		MAPK cascade activation	Applicable only to investigation of RTK-mediated pathways	70
BLUF domains								
euPAC	euPAC	FAD	Protein structure alteration	Mammalian cells, *Xenopus* oocytes, *Drosophila*	Blue	cAMP production	Large size of involved proteins, high background level in nonilluminated cells	73
bPac	bPAC			Mammalian cells, *Drosophila*			Applicable only to cAMP-dependent pathways	74
Cryptochromes								
CRY2-CIB1	CRY2	FAD	Heterodimerization of CRY2–CIBl	Mammalian cells	Blue	Protein translocation, transcription activation, Cre recombinase-mediated recombination	Applicable only to proteins that require oligomerization for activation	95

Optogenetic tool	Photoreceptor or domain	Chromophore	Mechanism of action	Expression system	Activation light	Type of application	Limitations	Reference(s)
5-ptase$_{OCRL}$						Regulation of phosphoinositide metabolism		79
CRY2			Homooligomerization of CRY2			Protein activation by clustering and oligomerization, cell morphology regulation	Reporter gene activates only under β-catenin-responsive elements control, applicable only to proteins that require oligomerization for activation	76
LARIAT			Homooligomerization of CRY2 combined with heterodimerization of CRY2–CIBl			Protein inactivation by cluster trapping	IgG-mediated inactivation of POI only in fusion with GFP	80
CRY2-C-RAF			Homooligomerization of CRY2			MAPK cascade activation	Applicable only to cRaf-dependent regulation pathways	77
LITE			Heterodimerization of CRY2–CIBl	Mammalian cells, mice		Gene expression modulation, epigenetic chromatin modifications	Large size of involved proteins	81
optoFGFRl			Homooligomerization of CRY2	Mammalian cells		Regulation of cell polarity and migration	Applicable only to studies of FGFR-mediated pathways	78
Phytochromes								
IlaC	BphGl	BV	Activation of effector domain exhibiting enzymatic function	*Caenorhabditis elegans*	NIR	Activation of cholinergic neurons by light induced synthesis of cAMP	Controls neurons by cAMP synthesis, is limited by time delay in response of system	82
LAPD	*Dr*BphP			Mammalian cells, zebrafish embryos		Regulation of cAMP or cGMP level by light-activated phosphodiesterase activity	Nonselectively catalyzes hydrolysis of both substrates	84
Light-switchable gene promoter system	PhyB, PhyA	PCB	Heterodimerization with PIF3	Yeast		Transcription activation	Requires exogenous PCB chromophore	88
Reversible interaction of PhyB with PIF6	PhyB		Heterodimerization with PIF6	Mammalian cells, chicken embryos, yeast		Control of protein-protein interaction, transcription activation		89, 90

Abbreviations: 5-ptase$_{OCRL}$, inositol 5-phosphatase domain of oculocerebrorenal syndrome of Lowe; *As*LOV2, *Avena sativa* light-, oxygen-, voltage-sensing domain2; bPac, *Beggiatoa* sp. photoactivated adenylyl cyclase; BphG1, *Rhodobacter sphaeroides* bacterial phytochrome; BV, biliverdin; cAMP, cyclic adenosine monophosphate; cGMP, cyclic guanidine monophosphate; CIB1, CRY-interacting bHLH1; C-RAF, rapidly accelerated fibrosarcoma kinase, isoform C; CRY2, cryptochrome 2; DAD, diaphanous autoregulatory domain; *Dr*BphP, *Deinococcus radiodurans* bacterial phytochrome; EL222, transcription factor from *Erythrobacter litoralis; El*LOV, *Erythrobacter litoralis* light-, oxygen-, voltage-sensing domain; euPAC, *Euglena gracilis* photoactivated adenylyl cyclase; FAD, flavin adenine dinucleotide; FGFR, fibroblast growth factor receptor; FKF1, flavin-binding kelch repeat F-box 1; FMN, flavin mononucleotide; GFP, green fluorescent protein; GI, GIGANTEA protein; IgG, immunoglobulin G; IlaC, IR light–activated adenylate cyclase; ipaA, vinculin-binding peptide from the invasin protein; L57V, light-inducible LOV domain–containing truncated mutant of caspase-7; LAD, light-activatable dimerizer; LAPD, light-activated phosphodiesterase; LightON, light-switchable transgene system; LITE, light-inducible transcriptional effectors; LITEZ, light-inducible transcription using engineered zinc-finger proteins; LARIAT, light-activated reversible inhibition by assembled trap; MAPK, mitogen-activated protein kinase; PA, photoactivatable; PAC (Pac), photoactivated adenylyl cyclase; PCB, phycocyanobilin; PhyA, phytochrome A; PhyB, phytochrome B; PIF3, phytochrome-interacting factor 3; PIF6, phytochrome-interacting factor 6; POI, protein of interest; Rac1, Ras-related C3 botulinum toxin substrate 1; RTK, receptor tyrosine kinase; SsrA, degradation-prone peptide from *Escherichia coli*; TULIP, tunable, light-controlled interacting protein tags; *Vf*LOV, *Vaucheria frigida* light-, oxygen-, voltage-sensing domain; VVD, *Neurospora crassa* Vivid protein; ZPF, zinc-finger protein.